

Some Technical Constraints on Possible
Tokamak Machines from Next Generation
to Reactor Size

A. Knobloch

IPP 4/133

November 1975



MAX-PLANCK-INSTITUT FÜR PLASMAPHYSIK

8046 GARCHING BEI MÜNCHEN

MAX-PLANCK-INSTITUT FÜR PLASMAPHYSIK
GARCHING BEI MÜNCHEN

Some Technical Constraints on Possible
Tokamak Machines from Next Generation
to Reactor Size

A. Knobloch

IPP 4/133

November 1975

Presented at the 6th Symposium on Engineering Problems
of Fusion Research, San Diego, November 18-21, 1975.

*Die nachstehende Arbeit wurde im Rahmen des Vertrages zwischen dem
Max-Planck-Institut für Plasmaphysik und der Europäischen Atomgemeinschaft über die
Zusammenarbeit auf dem Gebiete der Plasmaphysik durchgeführt.*

Some Technical Constraints on
Possible Tokamak Machines from
Next Generation to Reactor Size

A. Knobloch

November 1975

Abstract

A simplified consistent scaling of possible Tokamak reactors is set up in the power range of 0.1 - 10 GW. The influence of some important parameters on the scaling is shown and the role of some technical constraints is discussed. The scaling is evaluated for the two cases of a circular and a strongly elongated plasma cross section.

INTRODUCTION

Tokamaks are currently a much favoured concept in fusion research and they are in many countries the most advanced scheme in terms of size and technological complication. Recently, in the EEC the question of developing prototype coils and/or superconducting torus sector magnets as intermediate steps for the possibly required very large Tokamak magnets of the future has been discussed and currently a corresponding program is being set up. The real need for superconducting magnets in CTR Tokamak research seems only to come with what is called a feasibility machine which cannot yet be defined in detail. Because of the considerable time required for developing large fusion magnets it is widely accepted that such a program must start now.

It was for these reasons that the following simplified calculations were started in order to construct a framework of principal data and tendencies. In the course of the work it turned out also that technical constraints may strongly influence the choice of future Tokamak machine parameters.

It should be noted from the beginning that not the detailed numbers but the resulting tendencies can be expected to provide some guidelines among others for magnet development.

SCALING

The most relevant independent scaling parameter is the rated thermal power of a Tokamak fusion reactor when the basic assumptions on the reactor plasma are kept constant or kept in the same relationships. Given these a simplified geometric model yields the variation of the important parameters over a broad range of thermal powers. The latter

may be fictitious at low power levels in small machines because efficiencies, pulsed performance² and the dynamic behaviour of the plasma are not taken into account, but they still indicate the machine size considered.

An important item in capital cost of a Tokamak machine is the magnetic field system for which the stored energy is a rough measure. For purposes of comparison it is especially interesting to consider only the magnetic energy in the active reactor volume comprising the plasma and the blanket because this yields an absolute minimum of field energy required under the plasmaphysical assumptions given. The energy stored in a realistic toroidal magnet will be larger mainly for three reasons:

1. Very likely a poloidal divertor configuration has to fit inside the toroidal magnet.
2. Accessibility of the reactor chamber and maintenance and repair requirements call for additional space mainly at the outer torus magnet circumference.
3. Large coils will have to be shaped according to the electromagnetic forces such that minimum reinforcement against bending of the windings has to be provided.

Besides of the magnet energy a selected number of other important reactor parameters have been calculated from the scaling relationships.

The scaling has been carried out for both a circular and an elliptical plasma cross section to which the forms of the reactor chamber and the blanket were adapted. The torus magnet closely fits the outer contour of the blanket and as already mentioned comprises thus only the absolute minimum volume. The transformer winding has been idealized as a cylindrical coil closely fitting inside the torus and with a height equal to the blanket

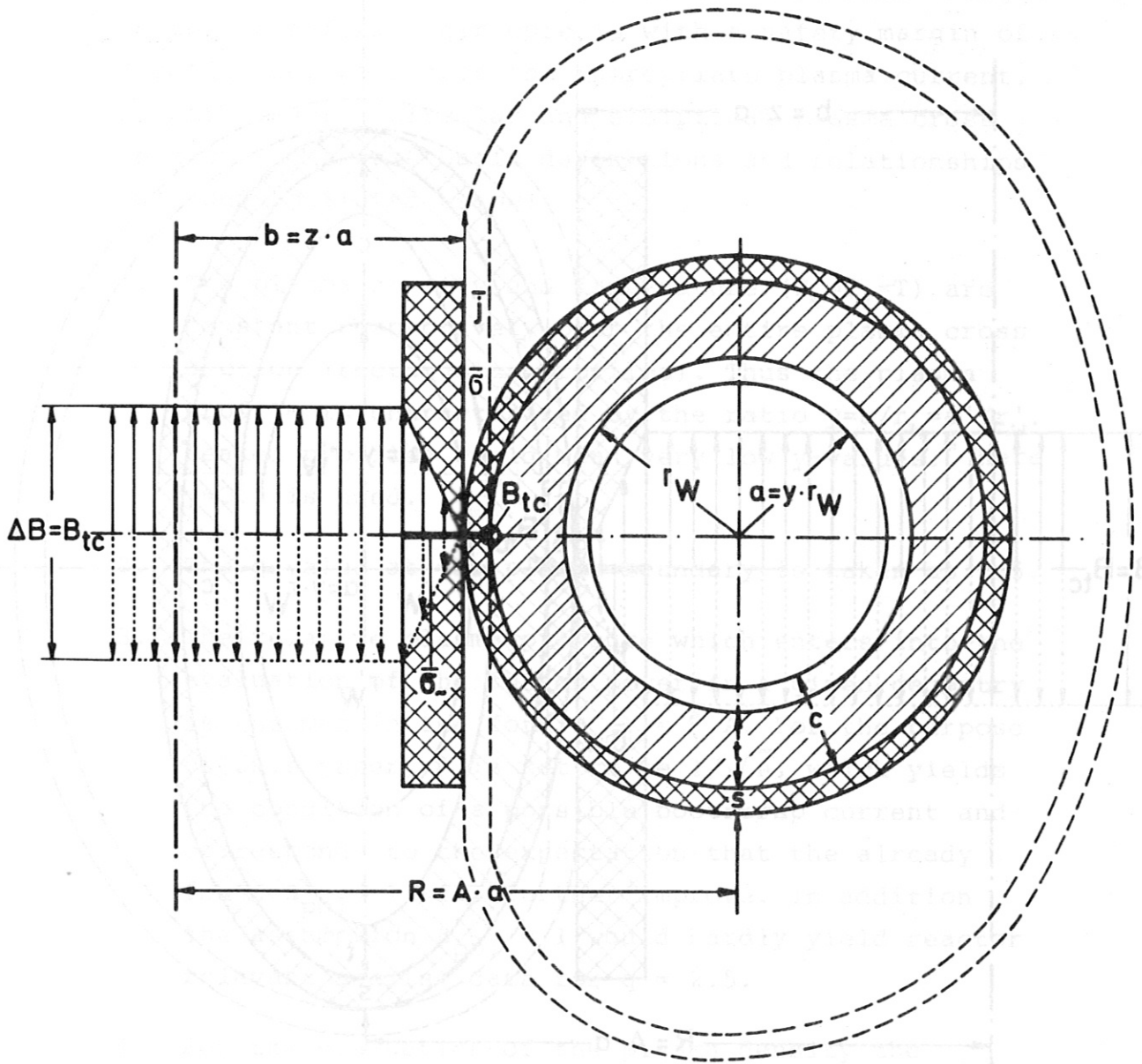


Fig. 1 Tokamak reactor-scaling model
Cylindrical cross section (CCS)

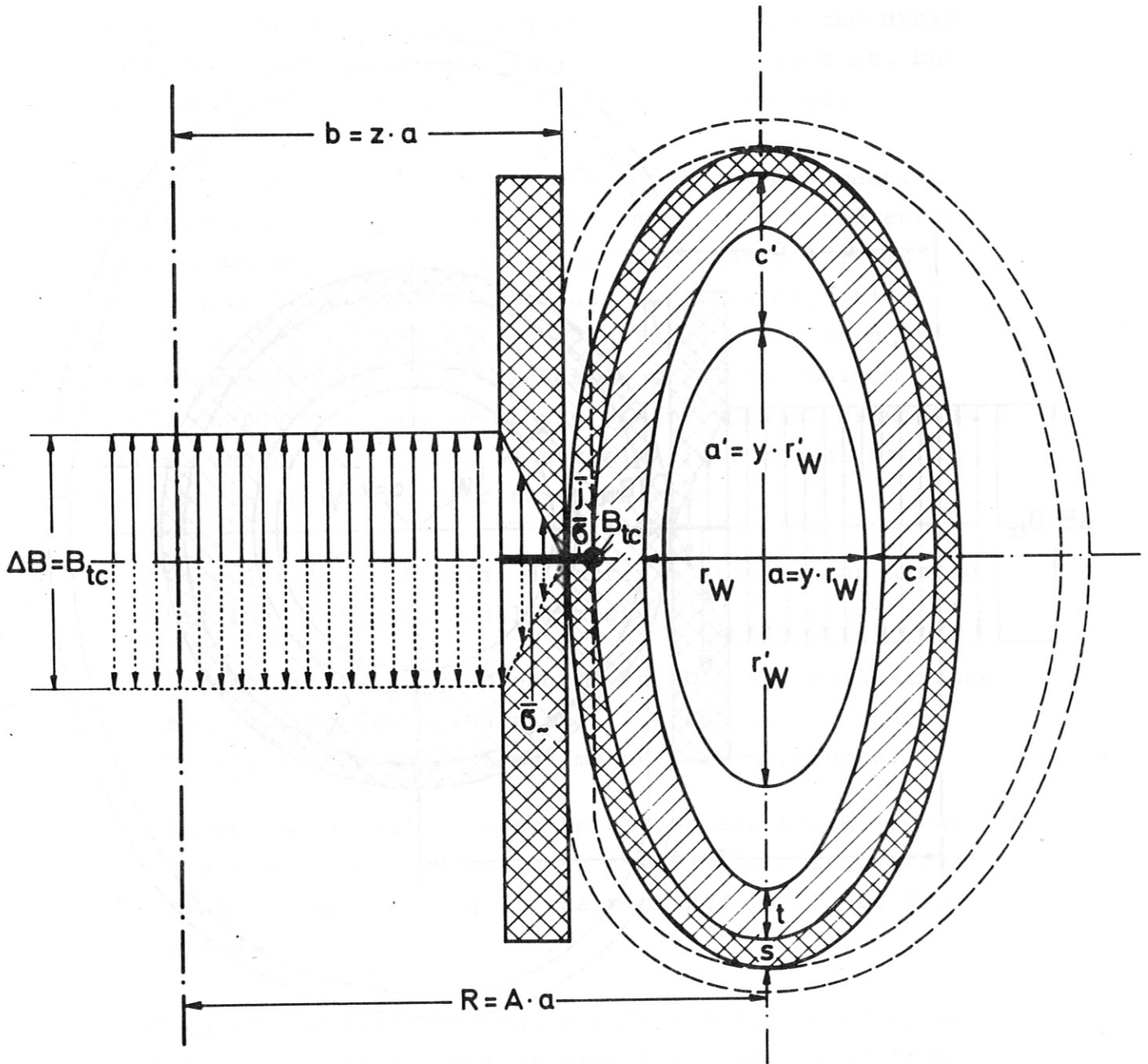


Fig. 2 Tokamak reactor-scaling model
Elliptical cross section (ECS)

vertical outer diameter. The bidirectional flux swing³ in the transformer air core is with a safety margin of 2 sufficient to induce the appropriate plasma current. In both cases - circular and elliptical plasma cross section - the same basic definitions and relationships are used as listed below:

1. The plasma density and temperature ($T_e=T_i=T$) are constant respectively over the entire plasma cross section (rectangular profiles). Thus the plasma profile is characterized by the ratio $y=a/r_w=a'/r_w'$. Peaked profiles would mean very low y -values.⁴ Here $y=0.9$ is used.
2. The q -value at the plasma boundary is taken as 2.5.
3. The relative plasma pressure which enters into the evaluation of the fusion power in a given geometry is assumed in the form $\beta_{pol} = \xi \cdot A$. For the purpose of this paper, ξ is set to be $1/\sqrt{A}$, which yields the condition of a possible bootstrap current and corresponds to the expectation that the already found $\beta_{pol} > 1$ will further improve. In addition the assumption $\beta_{pol} = 1$ would hardly yield reactor relevant scaling data for $q = 2.5$.
4. For the evaluation of the plasma density the temperature is assumed to be 20 keV.
5. The total fusion energy per event is taken to be $Q_{th} = 20$ MeV.
6. A total constant blanket thickness of $t = 200$ cm is assumed.
7. The radial thickness of the idealized transformer winding is calculated from an overall tensile stress of $\bar{\sigma} = 40$ MN/m² taking into account that a pulsating stress is applied. With this overall tensile stress value the question of overall and local current

density in the superconducting transformer winding should not present any problems.

8. The transformer flux density swing which is set equal to the maximum flux density in the torus magnet is chosen at $B_{tc} = 8 \text{ T}$, 12 T and 16 T in order to show the influence of the magnetic energy density. As mentioned above, the bidirectional flux swing has a safety margin of 2.
9. The radial thickness of the torus magnet winding s is calculated from three components. A first part takes the mechanical stress mainly in tension, a second part carries the current under the constraints of full stabilization and safety discharge at a given total voltage level, the third part is constant and represents the cryogenic insulation. Practically the functions will be at least partially interconnected, and only a rough picture is to be expected from this subdivision.

The tensile stress in the mechanical part is set at $\sigma = 400 \text{ MN/m}^2$ and the cryogenic part is set to be $d_c = 30 \text{ cm}$ in radial thickness.

10. The torus windings closely touch at the innermost circumference which calls for a common cryostat there. The effects of a discrete coil number are not yet taken into account. They lead to stronger tensile forces on the innermost part of the torus coils.
11. As has been derived elsewhere ⁵ the current density and the current in the superconducting toroidal magnet are calculated to meet the requirements of both the full stabilization and the safety discharge. The sum voltage over all the series connected coils at safety discharge is set at 200 kV. The temperature rise of the winding during safety discharge is set to be 50 K, thus $f(\theta)$ is $5 \cdot 10^8 \text{ (A/cm}^2\text{)}^2 \cdot \text{s}$. Further data are $q' = 0.3 \text{ W/cm}^2$ and $k = 2$, $\rho = 3 \cdot 10^{-8} \text{ } \Omega\text{cm}$.

12. The topological consistency of Fig. 1 and 2 is put into the scaling.

It should be noted that the scaling except for the above mentioned 12 items does not assume any dimension or other characteristic figure from the beginning. Especially the reactor power and the wall loading, the β -values, the density and the plasma current are not set from the beginning but are results of the scaling which yields under the many constraints imposed well defined dependences between realistic design parameters. There is no kind of optimization involved. Optimum data if any may be found in the results of the scaling.

Using constraint numbers 1, 2 and 6 through 12 one can derive an equation which in an implicit form provides $a = f(A)$ under the above conditions with the data for $y, q, t, \bar{g}, B_{tc}, \bar{g}, d_c, \Sigma V_{max}, \frac{a'}{a}$ set at certain values e.g. the ones mentioned in the text.

The equation reads

$$\sqrt[5]{\frac{\mu_0^6 \left(\frac{kq}{g}\right)^2 f(\theta) \Sigma V_{max}}{\pi^2 B_{tc}^7}} = \frac{\sqrt[5]{\frac{[Aa - (\frac{a}{y} + t)]^2 (\frac{a}{y} + t)^2 \frac{a'}{a}}{Aa}}}{s - \frac{B_{tc}^2}{2\mu_0 \bar{g}} (\frac{a}{y} + t) \left\{ \cdot \right\} - d_c} \quad (1)$$

where

$$s = (A - z)a - \left(\frac{a}{y} + t\right) \quad (2)$$

and

$$z = \sqrt{\frac{(\cdot) [Aa - (\frac{a}{y} + t)] \cdot [1 + (\frac{a'}{a})^2]}{2Aaq}} \left(4 + \frac{B_{tc}^2}{2\mu_0 \bar{g}}\right) \quad (3)$$

with

$$\left\{ \cdot \right\} = \frac{Aa - (\frac{a}{y} + t)}{(\frac{a}{y} + t)} \left[\frac{Aa + (\frac{a}{y} + t)}{2(\frac{a}{y} + t)} \ln \frac{Aa + (\frac{a}{y} + t)}{Aa - (\frac{a}{y} + t)} - 1 \right] \quad (4)$$

$$\text{and } (\%) = \left\{ \left[1 + \frac{(a')^2}{8A^2} \right] \ln \frac{A}{2\frac{a'}{a}} + \frac{9(a')^2}{32A^2} + 1,5 \right\} \left(1 - \frac{a}{a'} \right) + \left\{ \ln 8A \frac{a}{a'} - 1,75 \right\} \cdot \frac{a}{a'} \quad (5)$$

Equation (1) which only can be solved by iteration obviously relates the 9 constraints mentioned above. Equation (2) gives the radial overall winding thickness s of the torus coils. Equation (3) defines the relation between transformer core and plasma radii, equation (4) accounts approximately for the force distribution in the torus coils and equation (5) yields by interpolation between a thin belt shape and the torus shape ⁶ approximate inductance values for the elliptical plasma cross section with a ratio of long to short axis of a'/a .

The plasma aspect ratio

$$A = R/a \quad (6)$$

has the same meaning for both the circular and the elliptical case. a is either the plasma minor radius or the short axis of the ellipse. From $a = f(A)$ then introducing constraints 3 through 5 the fusion power relationships can be calculated. It is interesting to note that a relationship between the first wall total power flux density p_w and the absolute thermonuclear power P_{th} can be established without explicitly introducing the geometrical dimensions at first sight. ⁷

One finds

$$\frac{P_w^3}{P_{th}} = \frac{[Q_{th} \langle \sigma v \rangle]^2}{(16\mu_0)^4 \cdot \pi^2} \left(\frac{2}{1,5(1+\frac{a'}{a}) - \sqrt{\frac{a'}{a}}} \right)^3 \left(\frac{(a')^{10}}{2^8} \right) \left(\frac{B_{t_0}}{9} \right)^8 \frac{4^3 \cdot 5^4}{A^5} \quad (7)$$

where B_{t0} is the toroidal flux density on the plasma axis

$$B_{t0} = B_{tc} \left(1 - \frac{\frac{a}{y} + t}{Aa} \right) \quad (8)$$

and the expression $\left\{ \right\}$ becomes unity in the circular case.

As can be seen from equation (8) and also from the high power to which A enters into equation (7) the dimensions provided by $a = f(A)$ in fact already influence p_w^3/P_{th} rather strongly.

What can be seen however straight from equation (7) is that in a Tokamak the first wall loading is related to the absolute power and that this relation can be markedly influenced by the toroidal magnetic field strength, the plasma profile, the q-value, the ellipticity provided a'/a is larger than 2 and also of course by the β_{pol} -scaling.

Introducing $\xi = \frac{1}{\sqrt{A}}$ (9)
 which means $\beta_{pol} = \sqrt{A}$, equation (7) becomes

$$\frac{p_w^3}{P_{th}} = \frac{[Q_{th} \frac{\langle \sigma \gamma \rangle}{(kT)^2}]^2}{(16\mu_0)^4 \pi^2} \left(\frac{2}{1.5(1 + \frac{a'}{a}) - \sqrt{\frac{a''}{a}}} \right)^3 \left(\frac{(a')^{10}}{a} \right) \left(\frac{B_{t0}}{q} \right)^8 \frac{y^3}{A^7} \quad (10)$$

The expression $2 / [1.5(1 + \frac{a'}{a}) - \sqrt{\frac{a''}{a}}]$ approximates the relation of the circumference of a circle to the circumference of an ellipse. In both the circular and the elliptical case p_w is an average value taken over the entire first wall surface. Using equation (10) and the results of equation (1) one calculates for every pair $a = f(A)$

$$p_w = 2\pi a \sqrt{\frac{A}{y} \frac{1.5(1 + \frac{a'}{a}) - \sqrt{\frac{a''}{a}}}{2} \frac{p_w^3}{P_{th}}} \quad (11)$$

and from that

$$P_{th} = p_w^3 \left(\frac{P_m}{p_w^3} \right) \quad (12)$$

Now all the other Tokamak reactor parameters are available with consistent values:

Plasma current ⁸

$$J_p = \frac{B_{t0}}{\mu_0 q A} \cdot 2\pi a \frac{1 + \left(\frac{a'}{a}\right)^2}{2} \quad (13)$$

Plasma ring inductance

$$L_p \approx \mu_0 A a \cdot (\dots) \quad (14)$$

using equation (5) for (./.).

Toroidal field energy

$$W_{mt} \approx \frac{B_{t0}^2}{2\mu_0} 2\pi^2 A a \frac{a'}{a} \left(\frac{a}{y} + t + \frac{s}{3} \right)^2 \quad (15)$$

Toroidal magnet overall volume

$$V_{mt} \approx 4\pi^2 A a s \left(\frac{a}{y} + t \right) \frac{1,5 \left(1 + \frac{a'}{a}\right) - \sqrt{\frac{a'}{a}}}{2} \quad (16)$$

with equation (2) for s.

The total centering force can be roughly approximated by differentiation of the toroidal magnetic energy after the torus large radius which yields

$$F_c \approx \frac{B_{t0}^2}{2\mu_0} 2\pi^2 \frac{a'}{a} \left(\frac{a}{y} + t + \frac{s}{3} \right)^2 \quad (17)$$

An instructive measure for the design problems with the central support cylinders or rings is the centripetal pressure exerted on a fictitious cylinder surface with a radius of z.a. and a height equalling the vertical inner

diameter of the torus magnet. This centripetal pressure is given by

$$\sigma_c \approx \frac{B_{t_0}^2}{2\mu_0} \cdot \frac{\pi \left(\frac{a}{y} + t + \frac{s}{3}\right)^2}{2za \left(\frac{a}{y} + t\right)} \quad (18)$$

using equation (3) for z.

Another interesting figure is the total tilting force calculated for the worst case in which the vertical field according to ⁹

$$B_v = \mu_0 \frac{J_p}{4\pi Aa} (\ln A + \xi \cdot A + 0,83) \quad (19)$$

penetrates the whole torus magnet volume. The tilting force is taken to occur at the vertical inner diameter of the torus coils. Thus

$$\frac{M}{\frac{a'}{y} + t} = \frac{M}{a' + c'} \approx 2\pi Aa \left(\frac{a}{y} + t\right) \frac{B_v \cdot B_{t_0}}{\mu_0} \quad (20)$$

The average current density at the inner toroidal magnet circumference is

$$\bar{j} = \frac{B_{tc}}{\mu_0 s} \quad (21)$$

and the average tensile stress in the same region is

$$\bar{\sigma} = \frac{\bar{j} \cdot B_{tc}}{2} \left(\frac{a}{y} + t\right) \cdot \left\{ \frac{\cdot}{\cdot} \right\} \quad (22)$$

with equation (4) for $\left\{ \frac{\cdot}{\cdot} \right\}$.

Using these relationships and the constraints 9 and 11 the conductor current density, the current, the safety discharge voltage and time constant of the toroidal magnet are calculated.

$$j = \frac{\bar{j}}{1 - \frac{\bar{\sigma}}{\sigma} - \frac{d_c}{s}} \quad (23)$$

$$J = \left(\frac{Kq}{9} \right)^2 \frac{1}{j^3} \quad (24)$$

$$\sum V_{\max} = j^2 \frac{W_{mt}}{J \cdot f(\theta)} \quad (25)$$

$$\tau = \frac{2W_{mt}}{J \cdot \sum V_{\max}} \quad (26)$$

For the sake of simplicity in equation (1) the toroidal magnet energy has been introduced omitting $s/3$ in the minor toroidal magnet radius. Therefore the final sum voltage differs slightly from that put into equation (1) at the beginning.

Calculation of the consistent plasma density and β_t yields

$$n = \frac{\xi A}{A^2 q^2} \frac{B_{t_0}^2}{4\mu_0 kT} \left\{ \frac{1}{4} \left(\frac{a'}{a} \right)^2 \right\} \quad (27)$$

and

$$\beta_t = \frac{\xi A}{A^2 q^2} \left\{ \frac{1}{4} \left(\frac{a'}{a} \right)^2 \right\} \quad (28)$$

where $\left\{ \right\}$ is unity for the circular case.⁸

Using a very much simplifying equation¹⁰ one can estimate also roughly the scaling behaviour of Ohmic heating giving half the attainable temperature and the time to reach it:¹

$$kT_{\Omega} [\text{keV}] \approx 2,21 \cdot 10^{12} \cdot \frac{J_p}{\pi a^2 n} \frac{a}{a'} \quad (29)$$

and
$$\tau_{\Omega} [s] \approx 0,713 \cdot 10^{15} \frac{1}{n} \sqrt[4]{kT_{\Omega}} \quad (30)$$

Neutral heating requirements may be calculated from n.a. as well.

RESULTS

The equations derived above have been evaluated for the circular case and two elliptical cases with $a'/a = 2.5$ and 4. After a comparison of the resulting n and β_t scaling it must be concluded that for the fixed parameters chosen it is only interesting to consider $a'/a = 4$ as a possible alternative to the circular case. For $a'/a = 2.5$ the density and the plasma pressure are smaller than for a circular plasma cross section (Fig. 3).

In the following description and discussion of the results the circular and the elliptical case with $a'/a = 4$ are looked at in parallel.

Figures 4a and 4b show the scaling of the toroidal Tokamak magnets in terms of overall winding volume (including the space between single coils) versus magnet energy with the reactor power as a parameter varying between next generation (EPR) and reactor size. The important difference compared to present experimental machines, which causes a discontinuity in the scaling at about the EPR level, is the introduction of the blanket and shield. Therefore below the 0.1 GW level without a blanket much more favourable data may be generated, but they will not scale up.

From Fig. 4a and 4b it is interesting to note that depending on the maximum magnetic field strength the overall winding volume and in a certain region even the magnetic energy show a minimum at constant power. One could conclude that a maximum flux density of about 12 T at least in the circular case may offer some advantage over the lower and the higher field options. The elliptical configuration shows a less marked minimum behaviour, but at low power both the winding volume

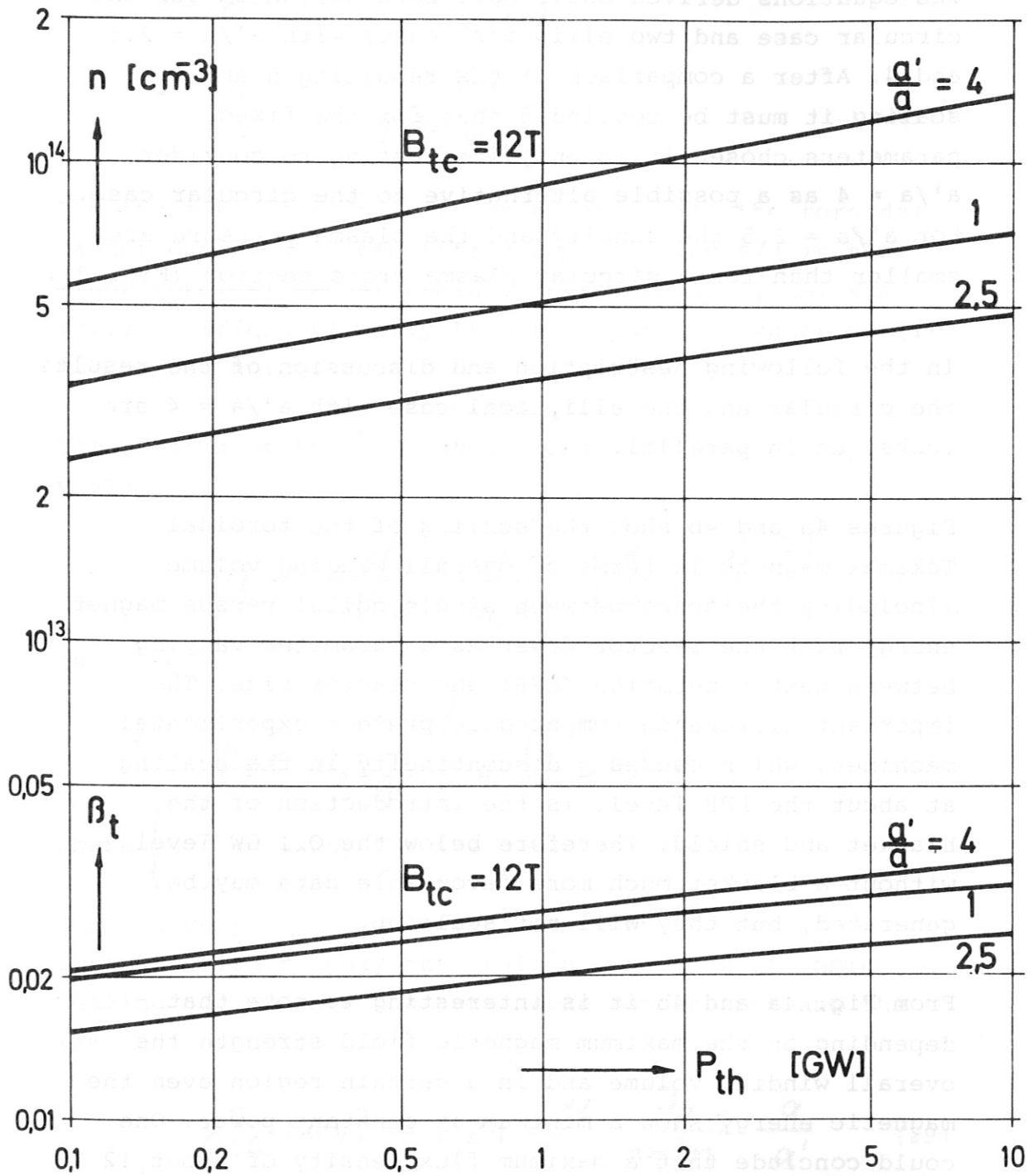


Fig. 3 Scaling of plasma density and β_t vs. reactor power for the circular case and two elliptical cases ($\frac{a'}{a} = 2.5$ and 4)

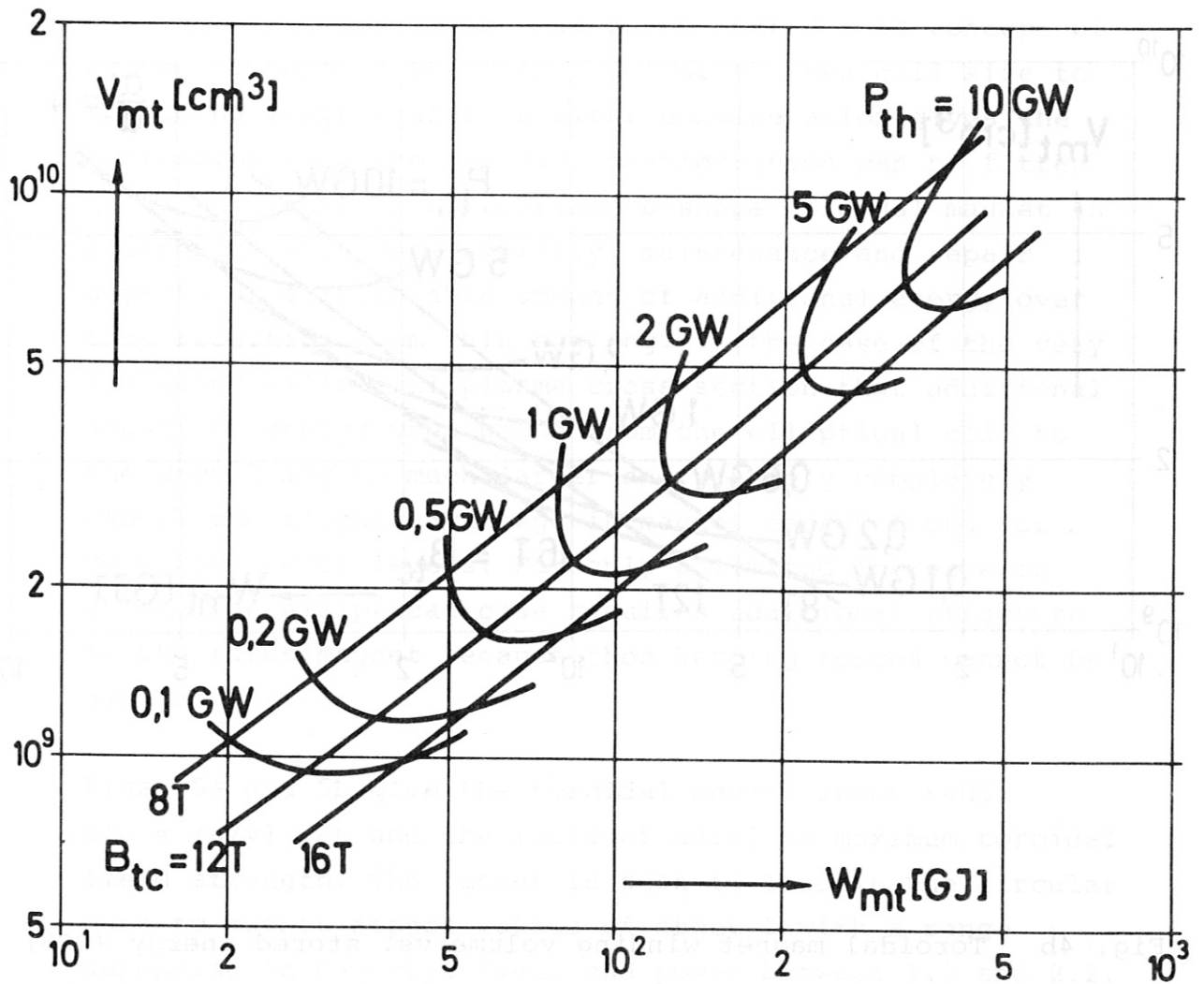


Fig. 4a Toroidal magnet winding volume vs. stored energy (CCS)

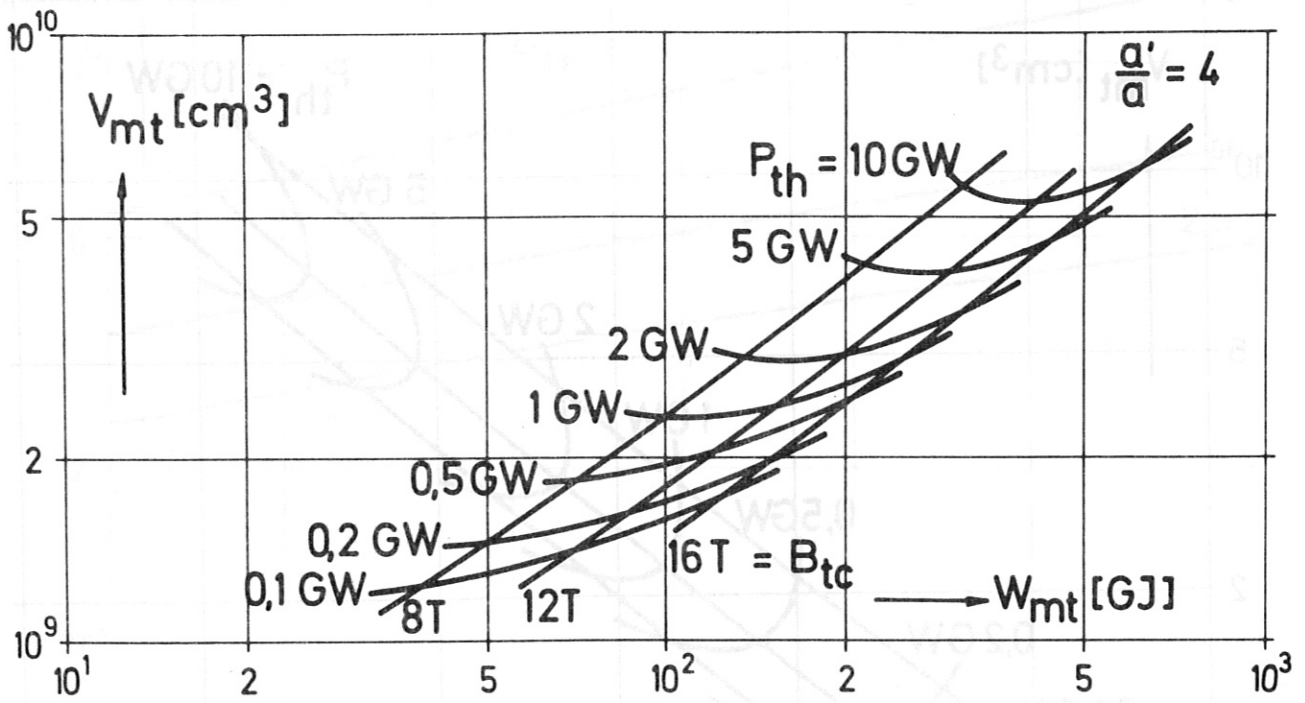


Fig. 4b Toroidal magnet winding volume vs. stored energy (ECS)

and magnet energy are much larger than in the circular case. Only at very high power levels the elliptical case yields lower volume and/or energy. As will be shown later, the elliptical configuration at $a'/a = 4$ has always a considerably higher wall loading compared to the circular one. Another problem is that the D-shaped coil concept of necessity relates the coil shape at a given coil size to the torus large radius. A first consideration gives the impression that the circular configuration can be fitted quite well into an appropriate D-shape toroidal magnet in accordance with accessibility, maintenance and repair aspects at a reasonable amount of additional energy over that resulting from this scaling. In the case of the very elongated elliptical plasma cross section that additional amount of energy when going from the elliptical coil to the D-coil may be much larger and possibly completely cancel the slight advantage in magnet energy found for very high power levels. For only a limited increase in energy the elliptical case requires additional structure in the torus magnet because then bending forces cannot be avoided.

Figs. 5a and 5b give the toroidal magnet inner radii $a+c = (a/y) + t$ and the ratio of axial to maximum toroidal field strength. The latter is seen to lead in the circular case to magnet aspect ratios of about 2 with a range depending on magnetic field and power between 1.7 and 2.2. At $a'/a = 4$ the field dependence is very small and the magnet aspect ratio varies between 2.1 and 3.1. This indicates the influence of the higher plasma current in the elliptical case.

When plotting the toroidal magnetic energy versus the magnet aspect ratio A_m (see Figs. 6a and 6b) the constraints imposed on the magnet clearly appear

$$[A_m = 1/(1-B_{t0}/B_{tc})].$$

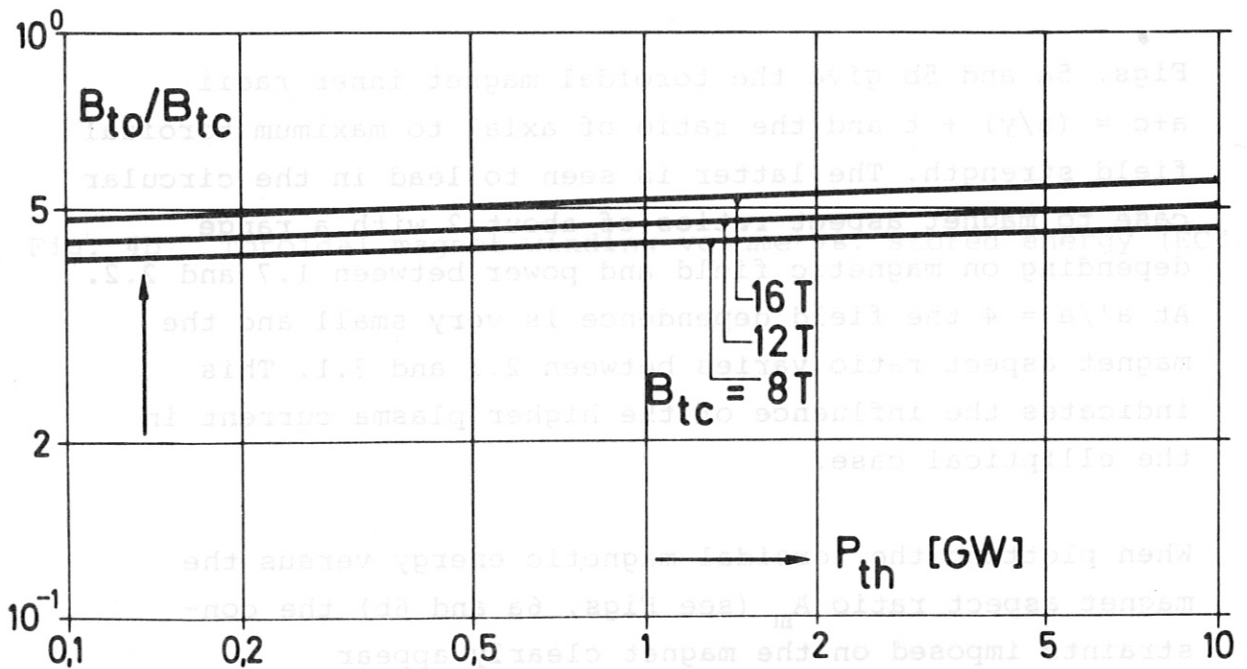
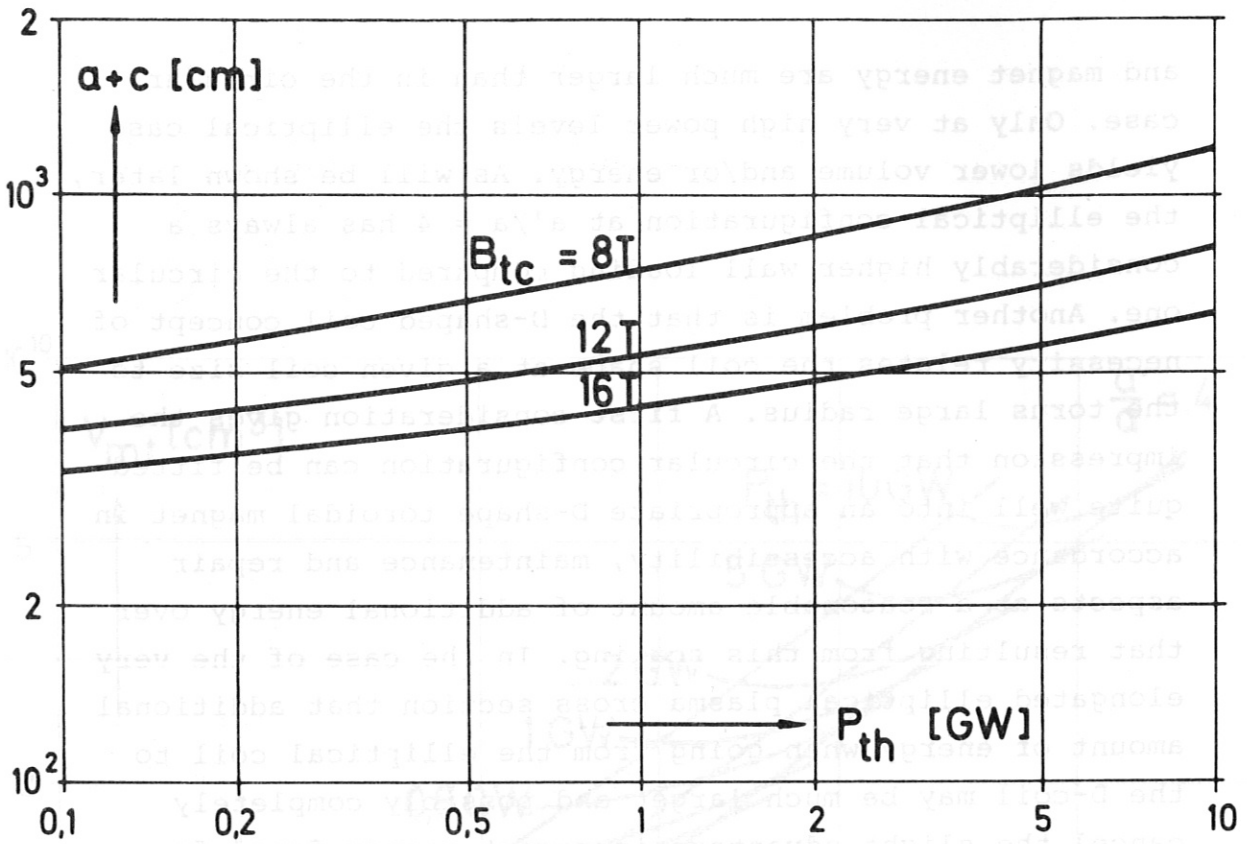


Fig. 5a Toroidal magnet inner radii and B_{t0}/B_{tc} vs. reactor power (CCS)

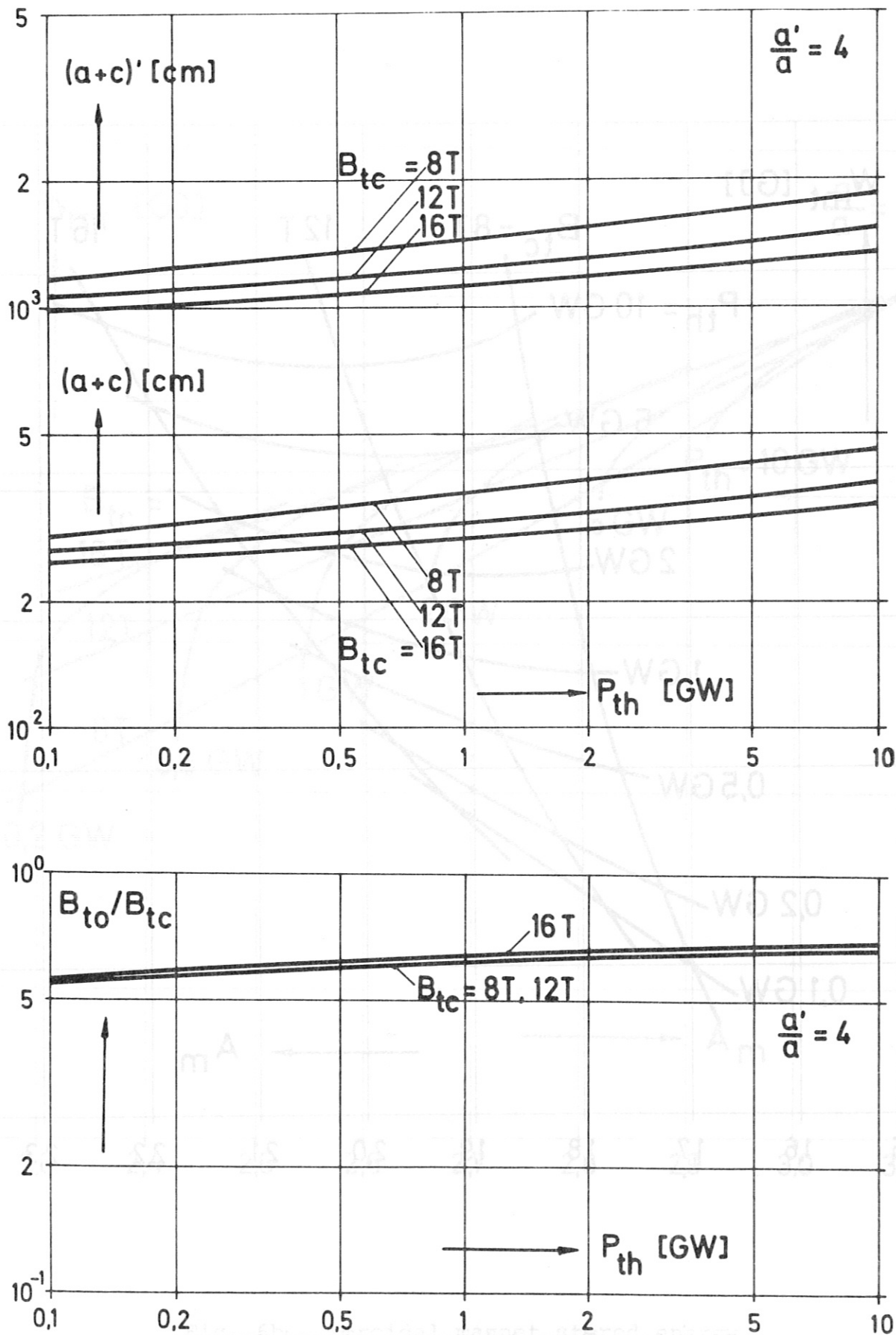


Fig. 5b Toroidal magnet inner radii and B_{to}/B_{tc} vs. reactor power (ECS)

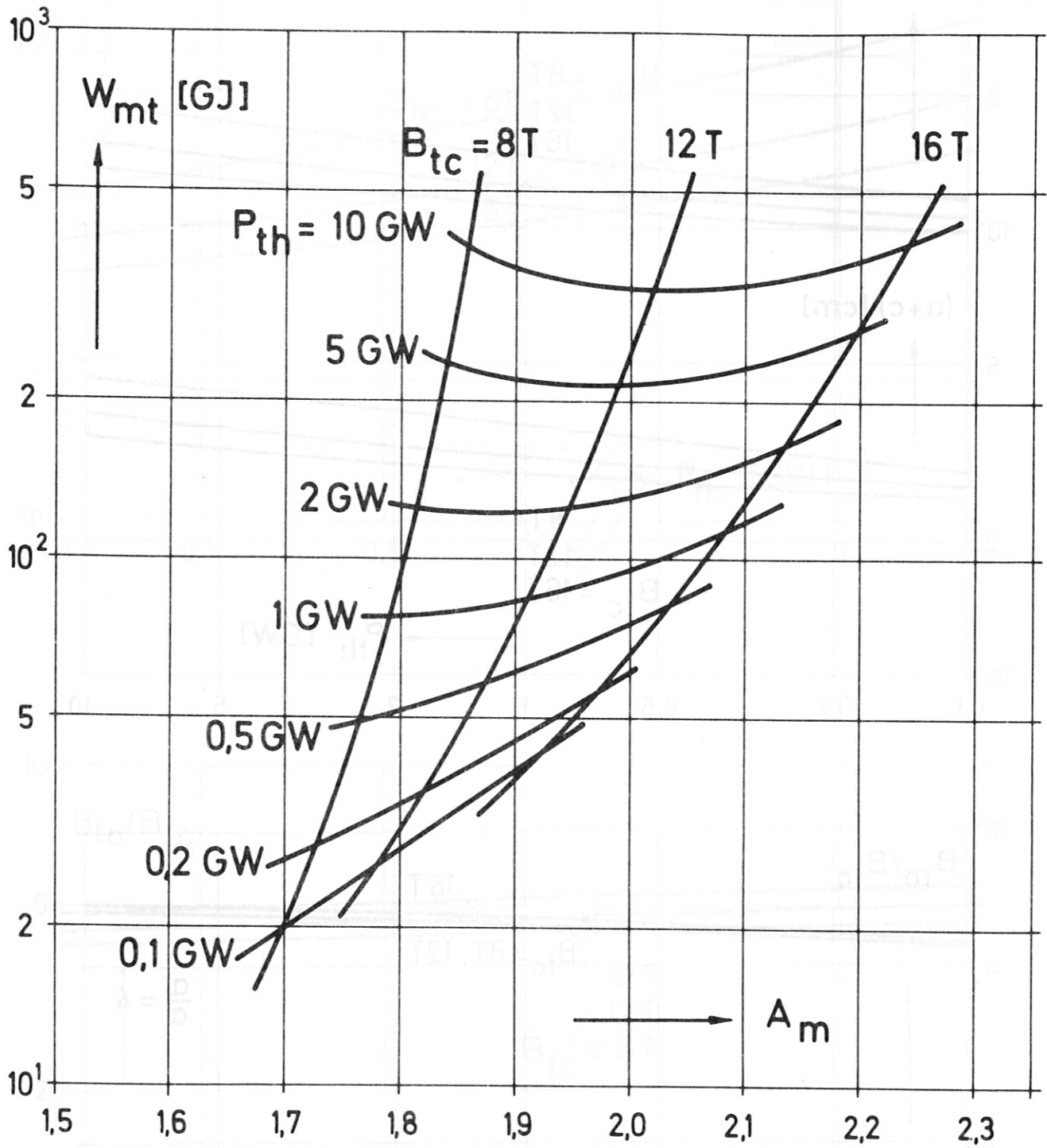


Fig. 6a Toroidal magnet stored energy vs. magnet aspect ratio (CCS)

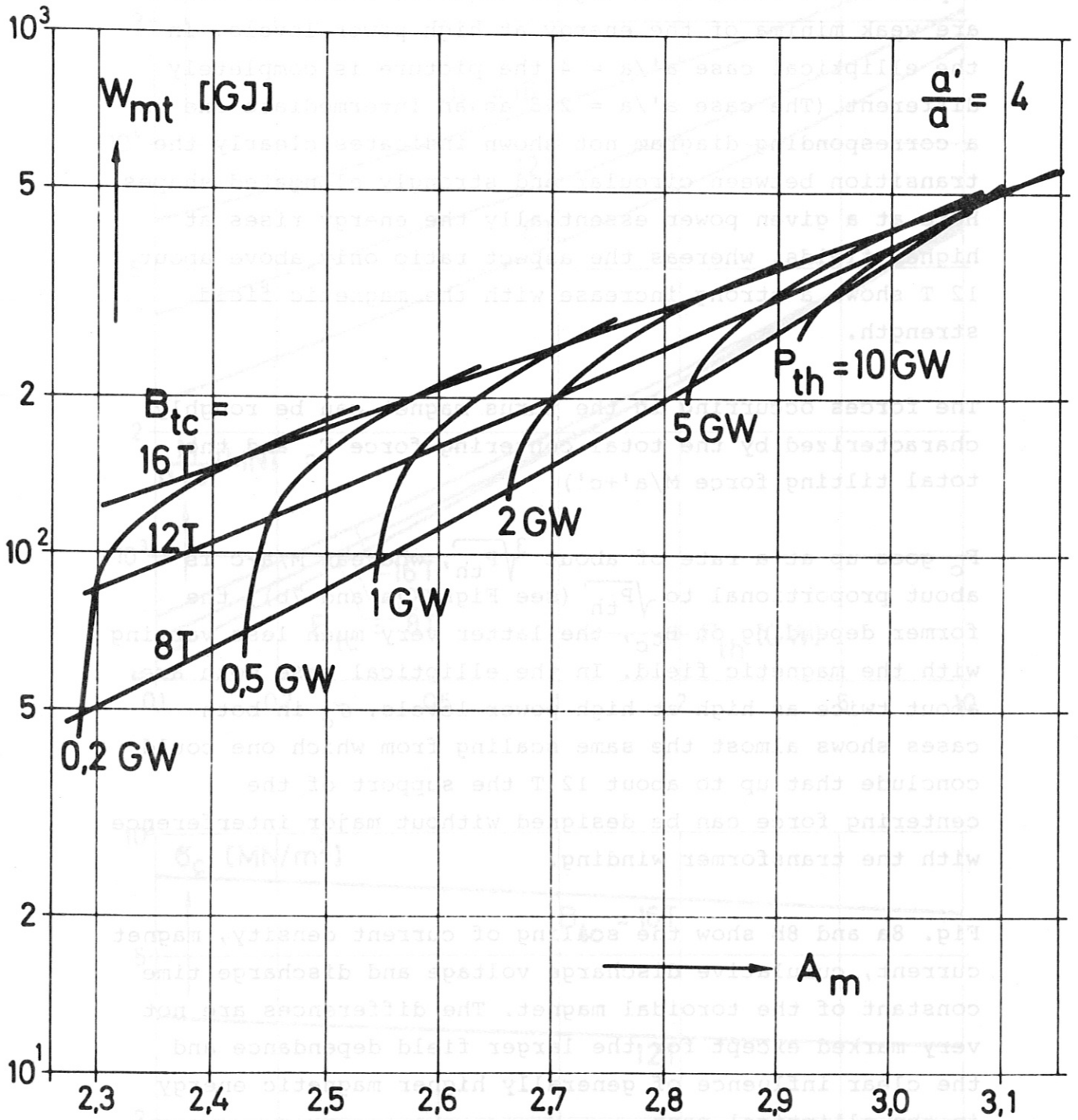


Fig. 6b Toroidal magnet stored energy vs. magnet aspect ratio (ECS)

In the circular case at a given power essentially the aspect ratio rises with higher magnetic field and there are weak minima of the energy at high power levels. In the elliptical case $a'/a = 4$ the picture is completely different (The case $a'/a = 2.5$ as an intermediate one in a corresponding diagram not shown indicates clearly the transition between circular and strongly elongated shapes). Here at a given power essentially the energy rises at higher fields, whereas the aspect ratio only above about 12 T shows a strong increase with the magnetic field strength.

The forces occurring in the torus magnet can be roughly characterized by the total centering force F_c and the total tilting force $M/a'+c'$.

F_c goes up at a rate of about $\sqrt[3]{P_{th}}$, whereas $M/a+c$ is about proportional to $\sqrt{P_{th}}$ (see Figs. 7a and 7b), the former depending on B_{t_c} , the latter very much less varying with the magnetic field. In the elliptical case both are about twice as high at high power levels. σ_c in both cases shows almost the same scaling from which one could conclude that up to about 12 T the support of the centering force can be designed without major interference with the transformer winding.

Fig. 8a and 8b show the scaling of current density, magnet current, cumulative discharge voltage and discharge time constant of the toroidal magnet. The differences are not very marked except for the larger field dependence and the clear influence of generally higher magnetic energy in the elliptical case.

Figs. 9a and 9b connect the technical data to the plasma physical ones. The plasma radius and the torus magnet energy are drawn versus the plasma aspect ratio for $\gamma = 0.9$, $q = 2.5$ and $\beta_{pol} = \sqrt{A}$. The upper diagrams show the solution of equation (1) and by comparison it is

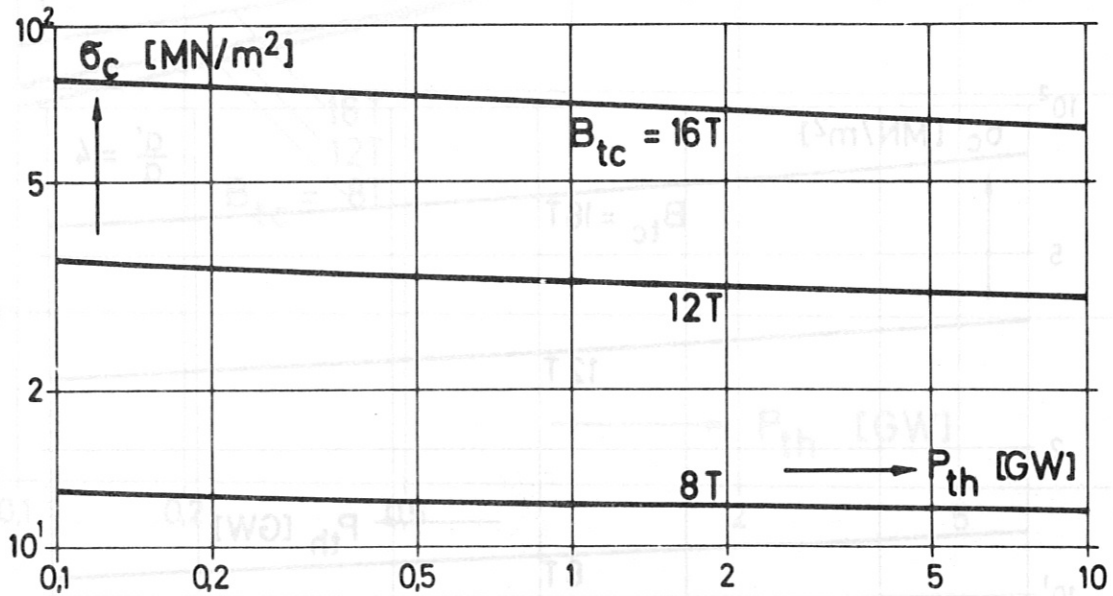
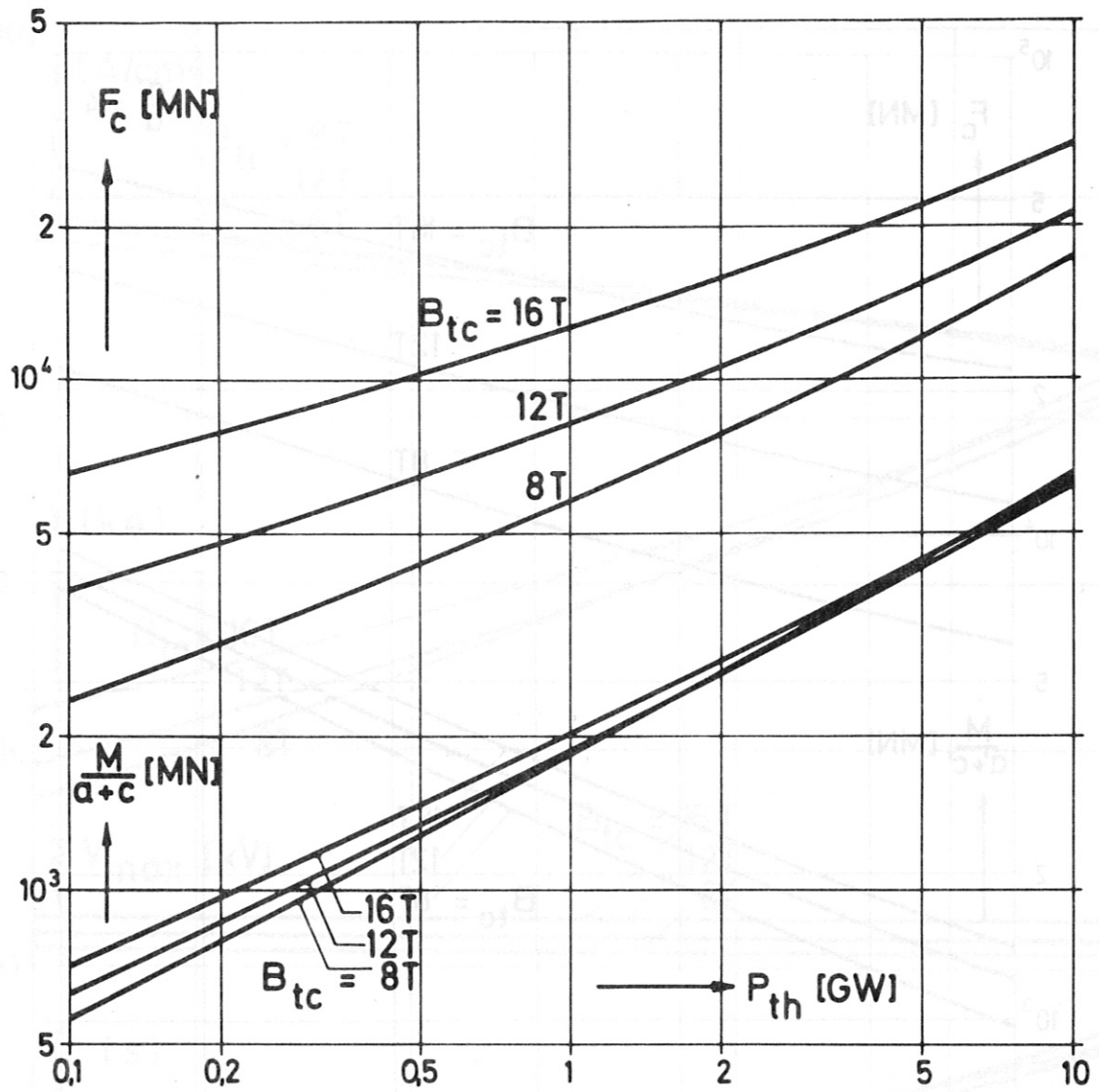


Fig. 7a Toroidal magnet centering and tilting forces vs. reactor power (CCS)

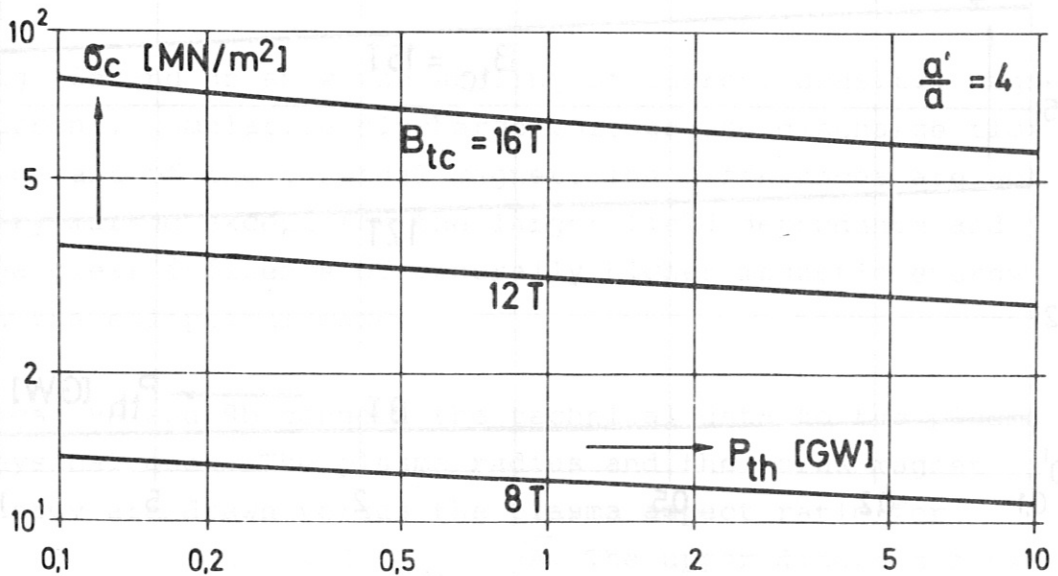
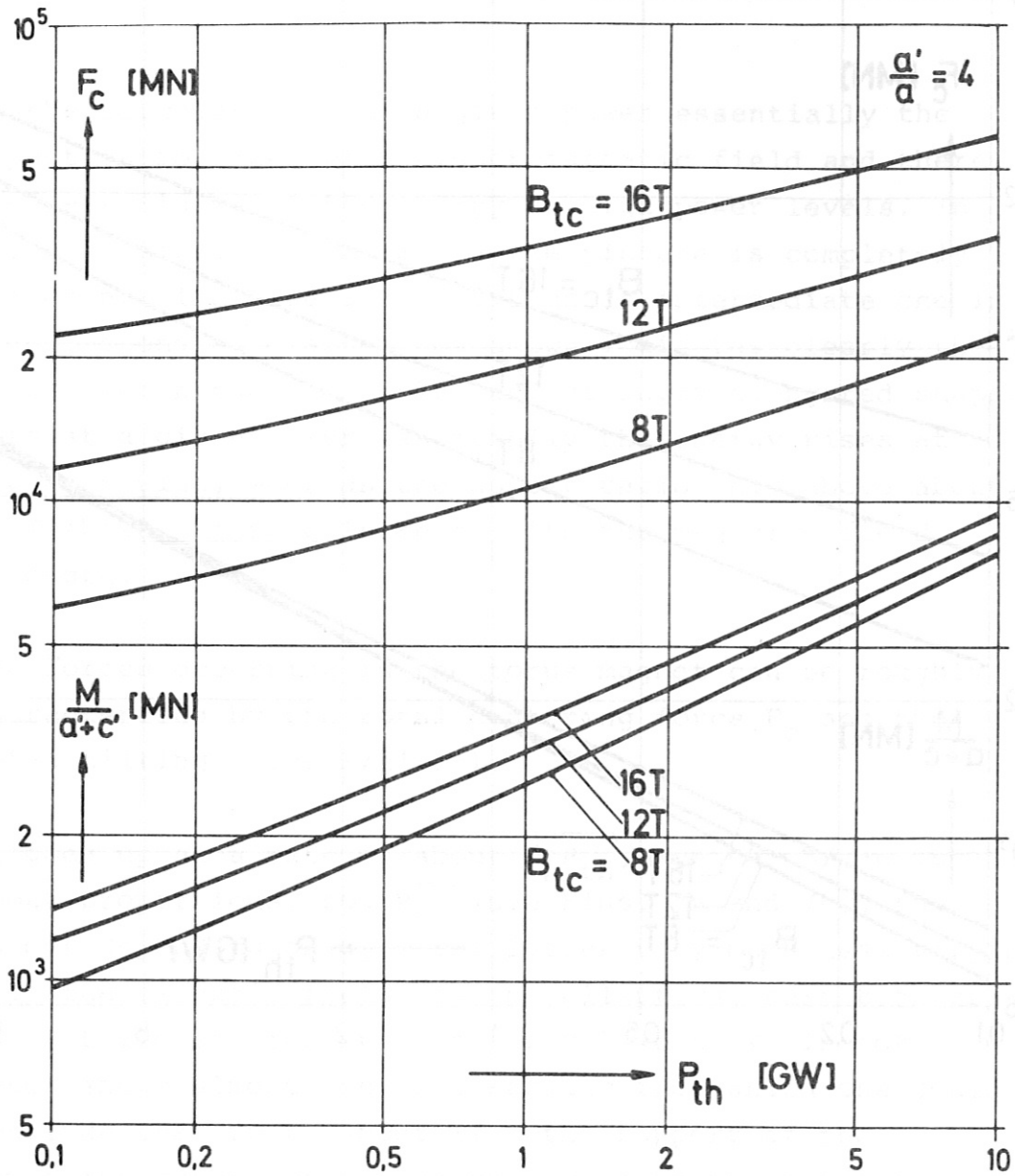


Fig. 7b Toroidal magnet centering and tilting forces vs. reactor power (ECS)

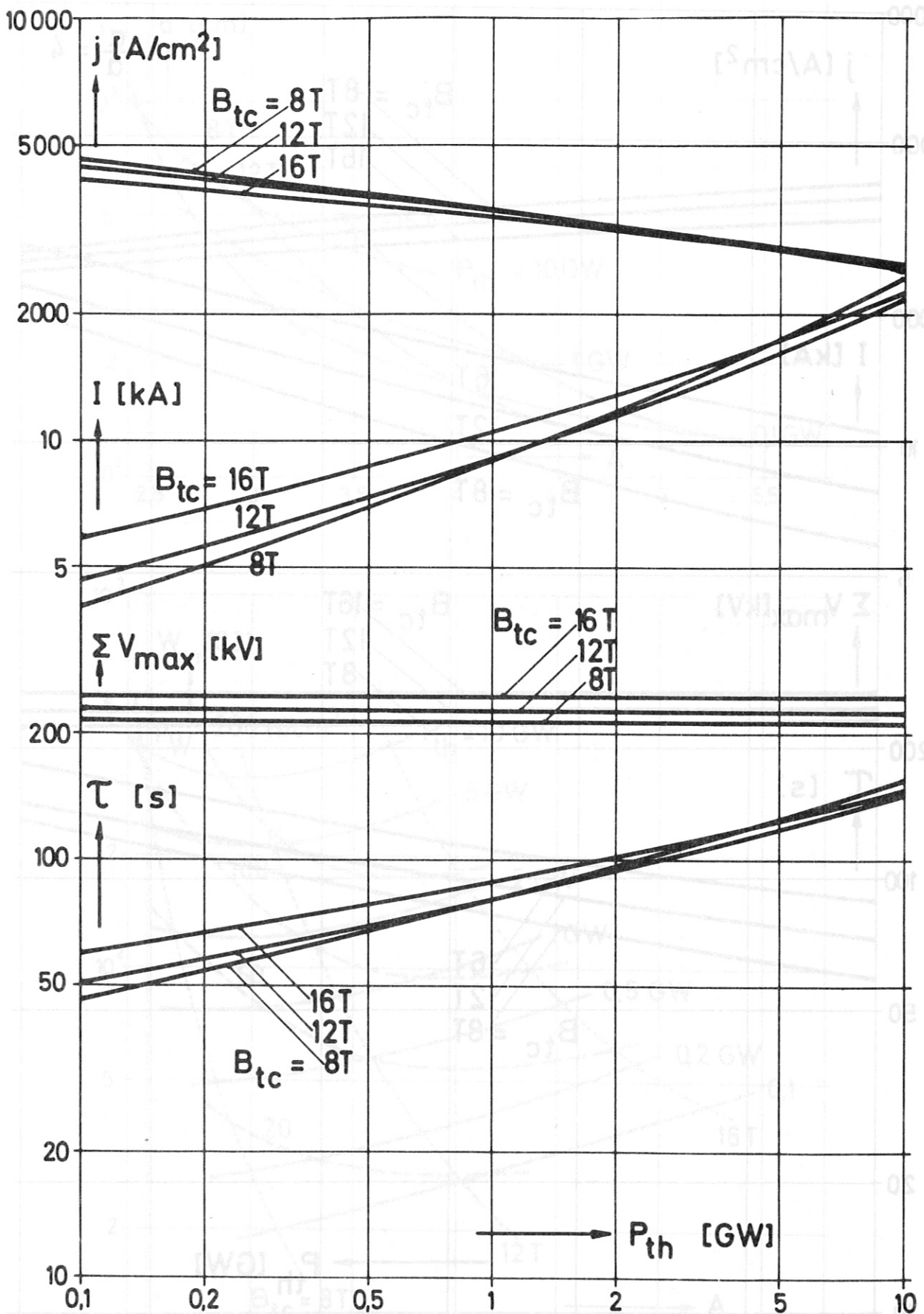


Fig. 8a Toroidal magnet current density, current, discharge voltage and time constant vs. reactor power (CCS)

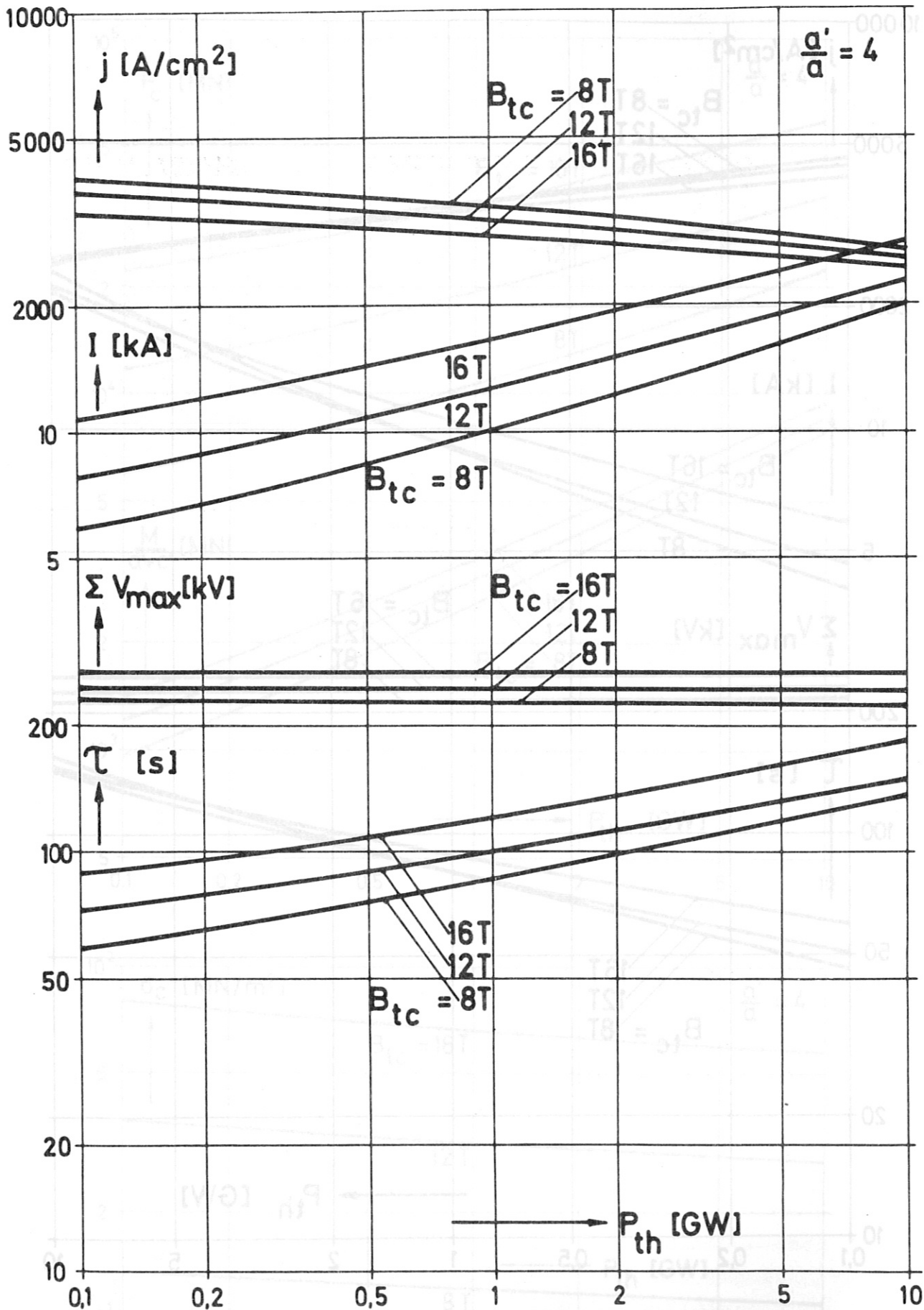


Fig. 8b Toroidal magnet current density, current, discharge voltage and time constant vs. reactor power (ECS)

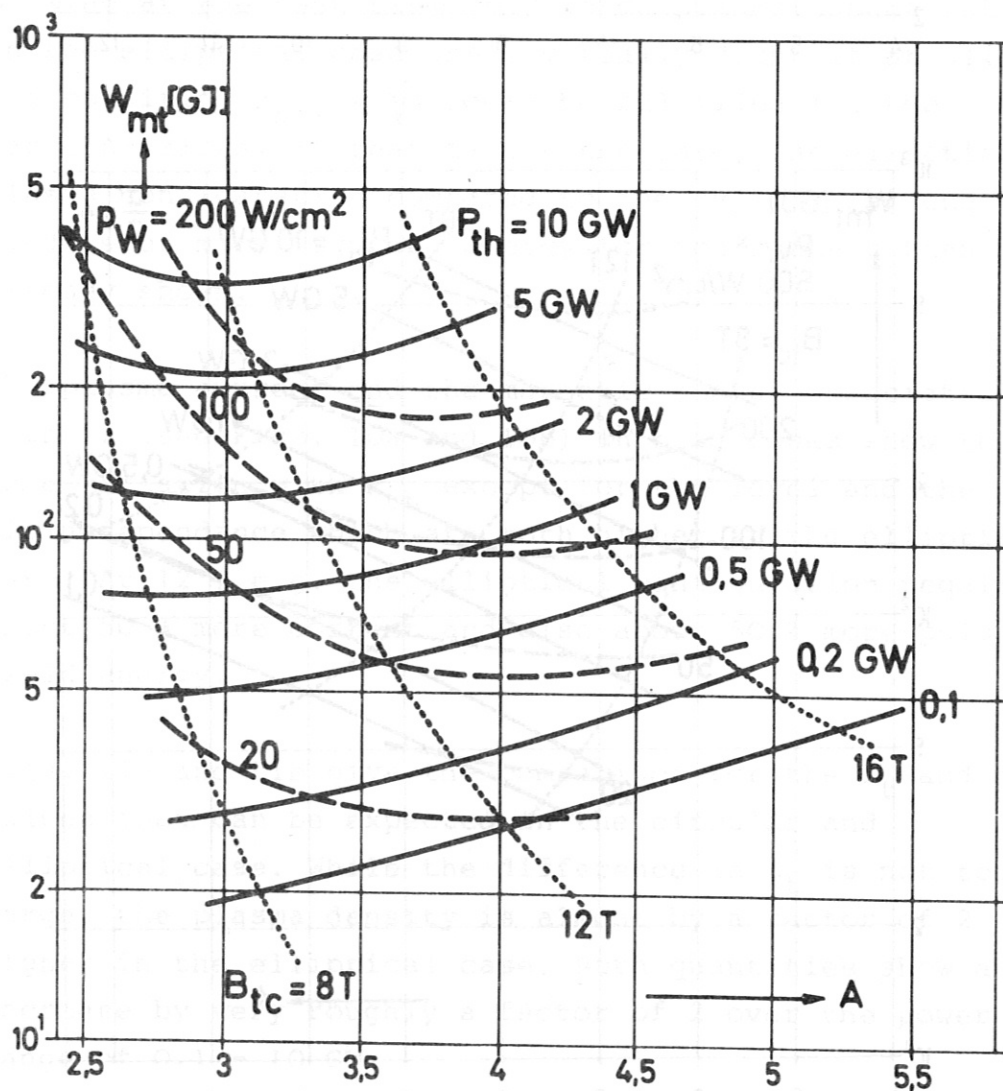
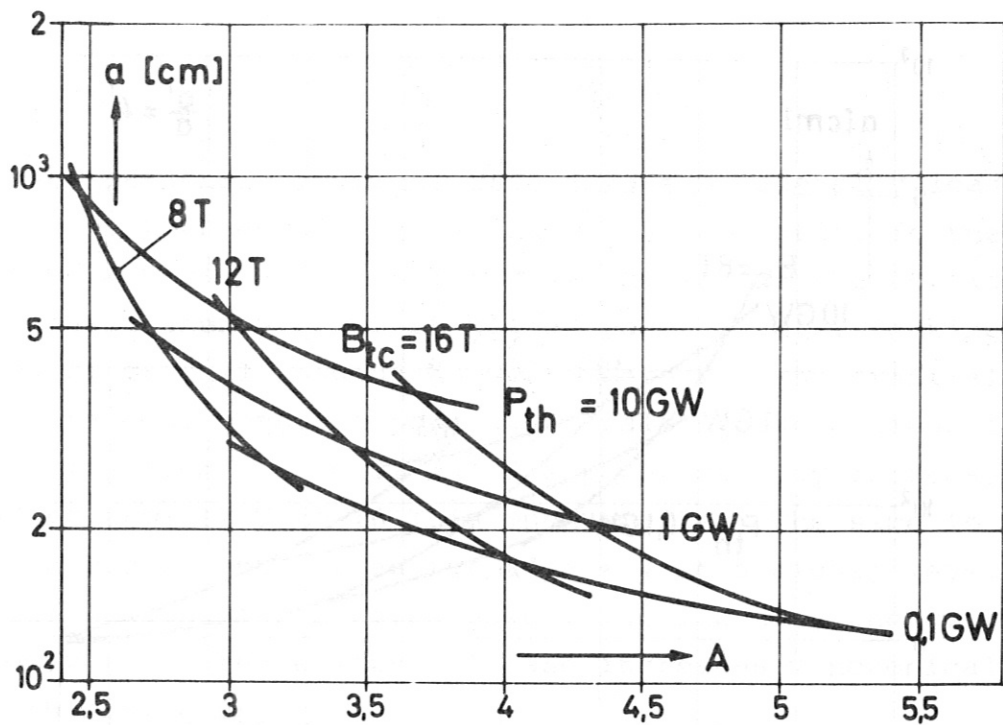


Fig. 9a Plasma radius and toroidal magnet stored energy vs. plasma aspect ratio for $\gamma = 0.9$, $q = 2.5$, $B_{pol} = \sqrt{A}$ (CCS)

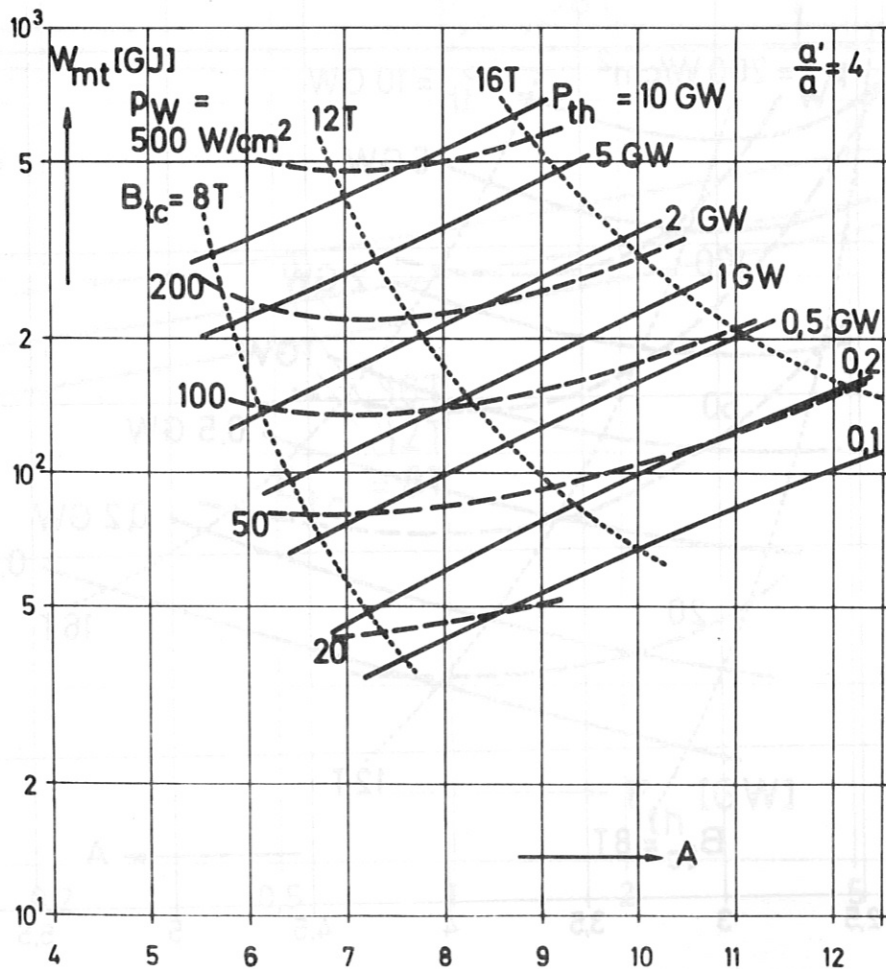
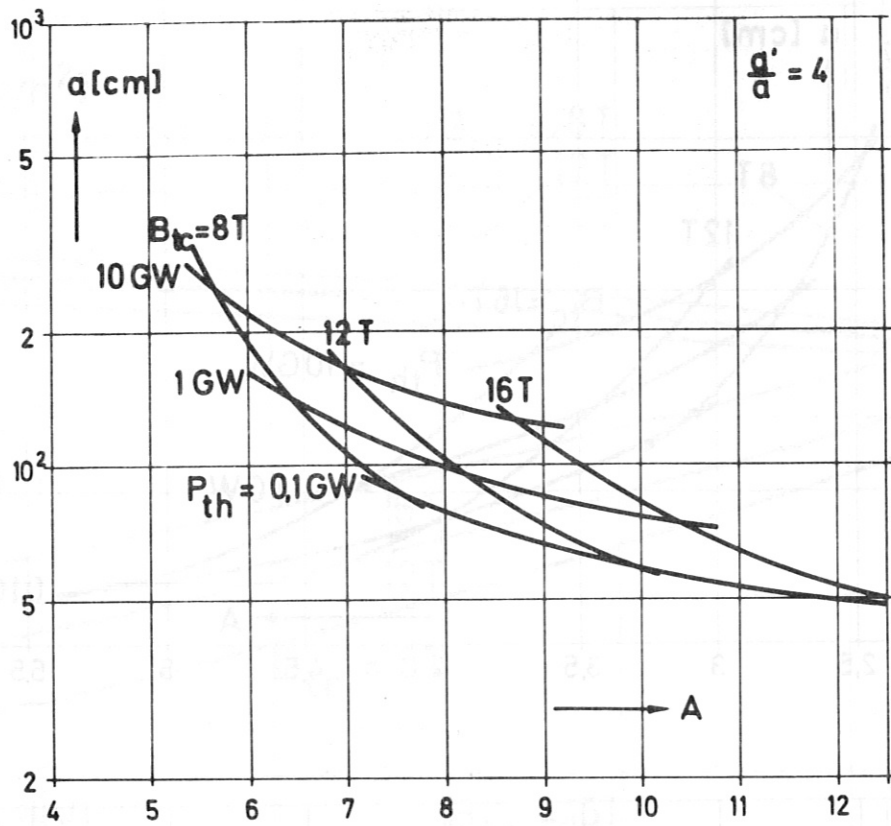


Fig. 9b Plasma radius and toroidal magnet stored energy vs. plasma aspect ratio for $\gamma = 0.9$, $q = 2.5$, $\beta_{pol} = \sqrt{A}$ (ECS)

seen that the elliptical case $a'/a = 4$ generally leads to more than doubling the plasma aspect ratio. In the circular case at about 12 T weak minima of the toroidal magnetic energy occur at higher power levels. Looking at the first wall loading however there is a substantial increase at constant power when raising the maximum flux density from 8 T to 12 T. The power density increase in going from 12 T to 16 T is much smaller. The same is observed in the curves for $a'/a = 4$ at a higher level of wall loading for a given power. The magnetic energy, however, in the elliptical case increases monotonically with rising Bt_c .

Looking at the resulting very large plasma aspect ratios in the elliptical case one may really doubt if at all the condition $\beta_{pol} = \sqrt{A}$ could be fulfilled for the large A-values. If that is not the case, the elliptical plasma configuration compared to the cylindrical one needs even more magnetic energy for confinement than already shown.

The plasma current and the magnetic energy associated with it (see Figs. 10a and 10b) in both cases show the same variation with P_{th} except for the level and the field dependence which are both higher in the elliptical case. At 12 T e.g. the elliptical configuration requires about 50 % more current and also about 50 % more poloidal field energy.

Figs. 11a and 11b give the comparison for the β_t and n values that can be expected in the circular and elliptical case. While the difference in β_t is not too large, the plasma density is almost by a factor of 2 higher in the elliptical case. Both quantities show an increase by very roughly a factor of 2 over the power range of 0.1 - 10 GW.

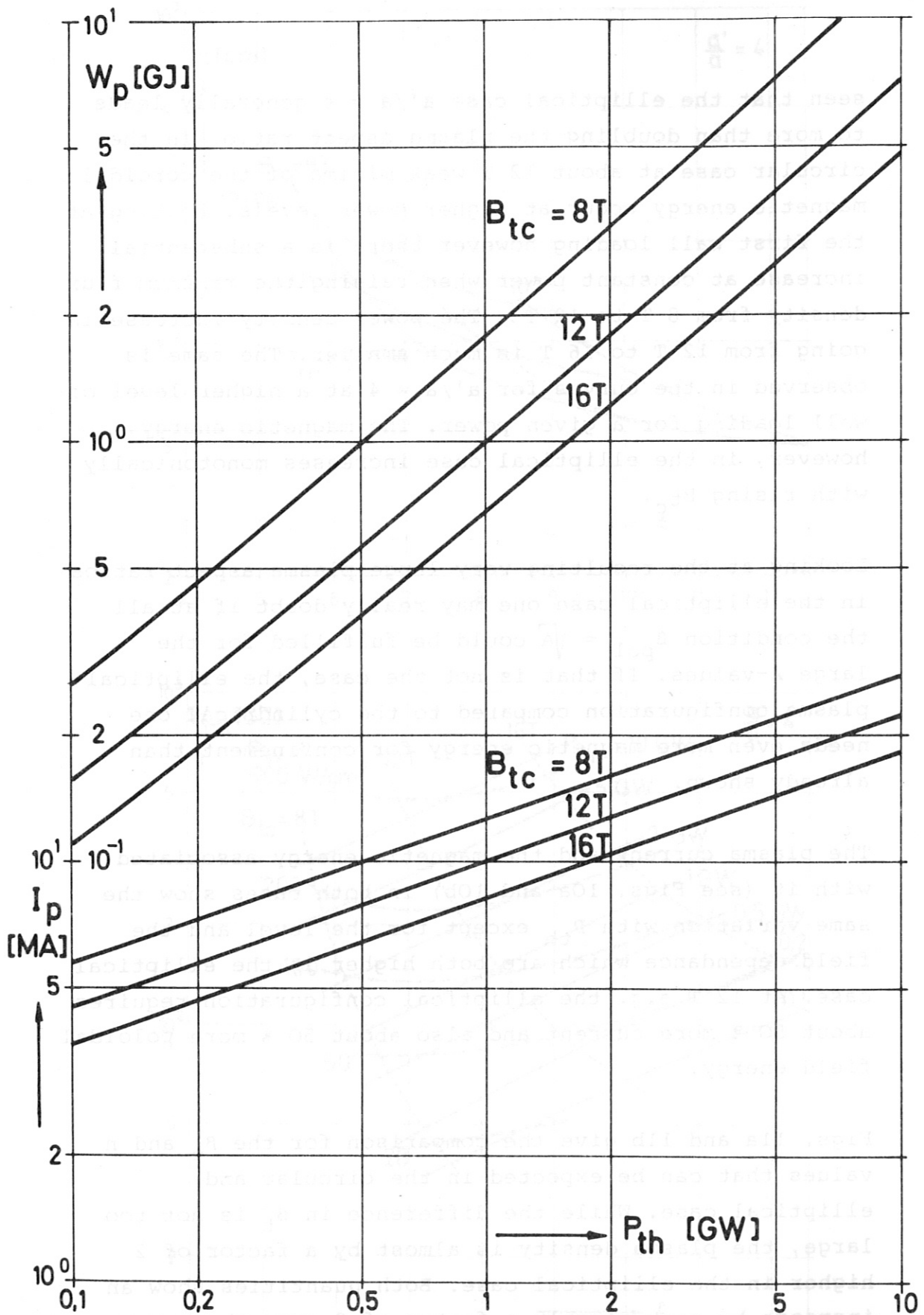


Fig. 10a Plasma current and poloidal magnetic energy vs. reactor power (CCS)

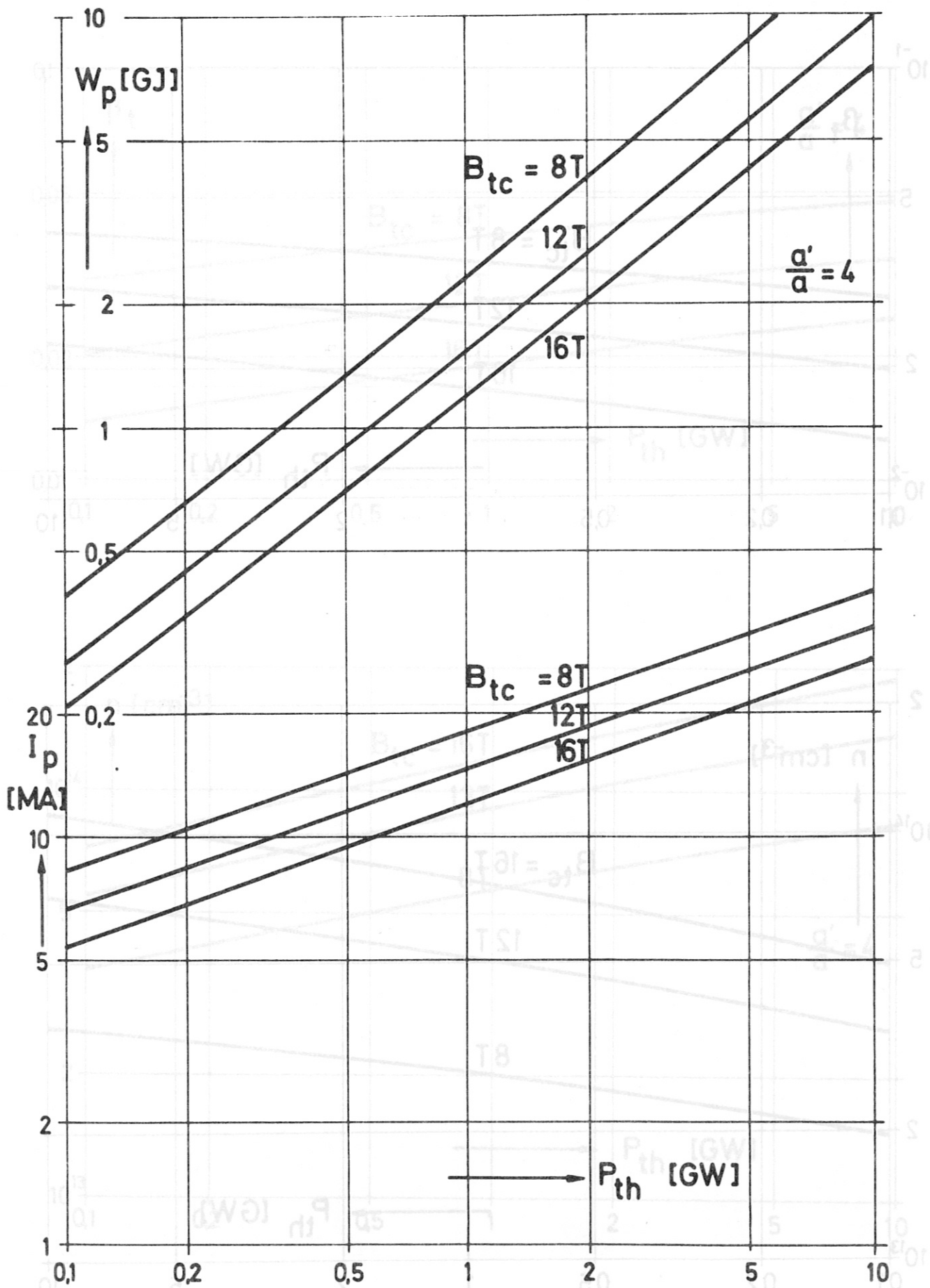


Fig. 10b Plasma current and poloidal magnetic energy vs. reactor power (ECS)

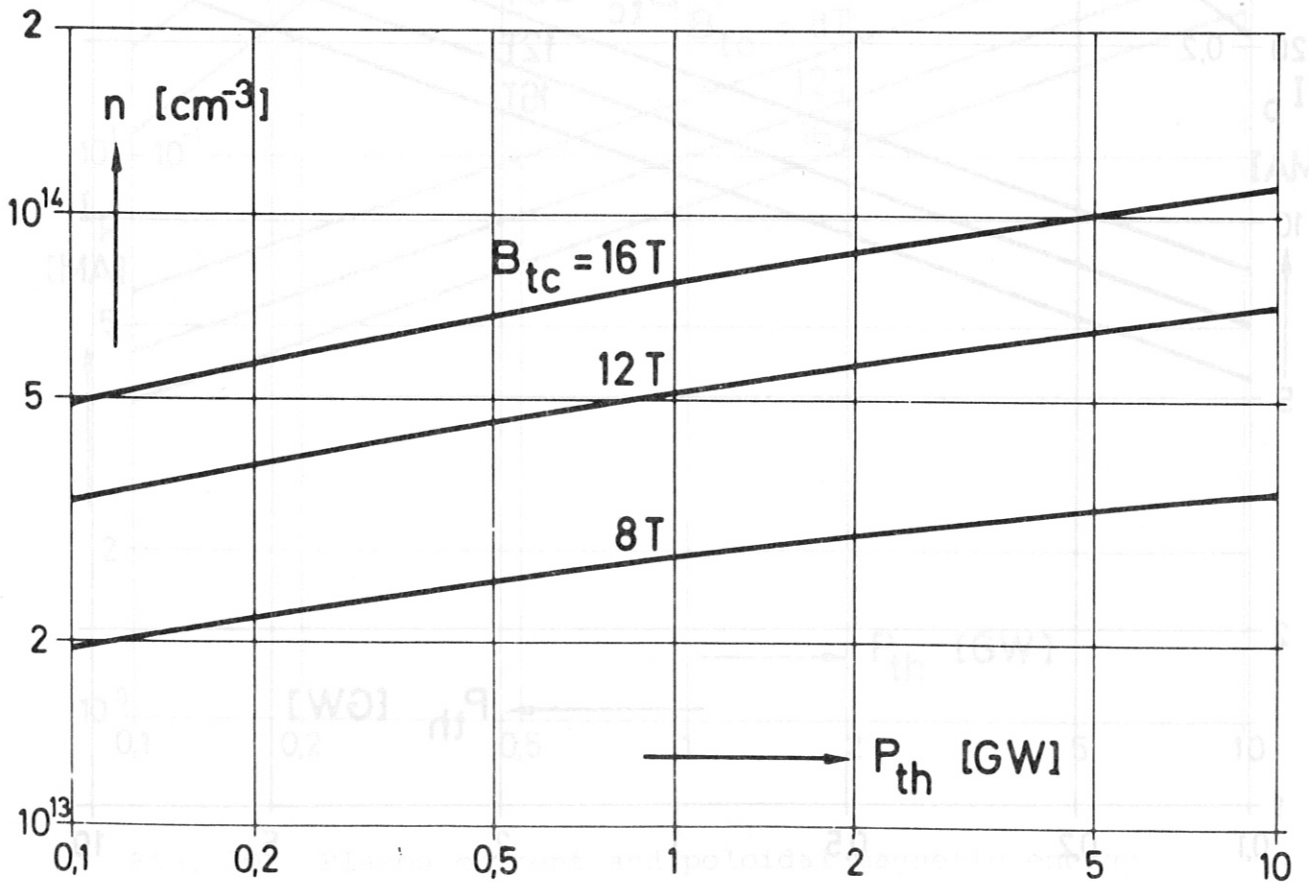
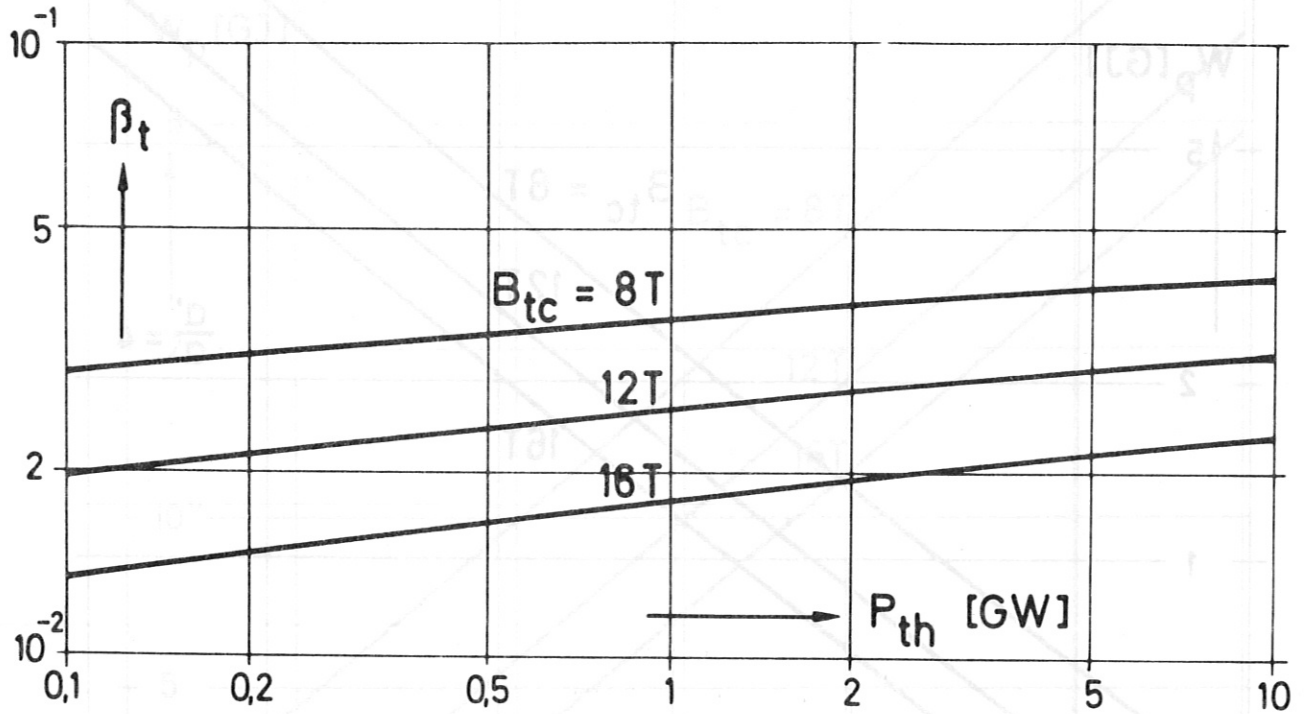


Fig. 11a β_t and plasma density vs. reactor power (CCS)

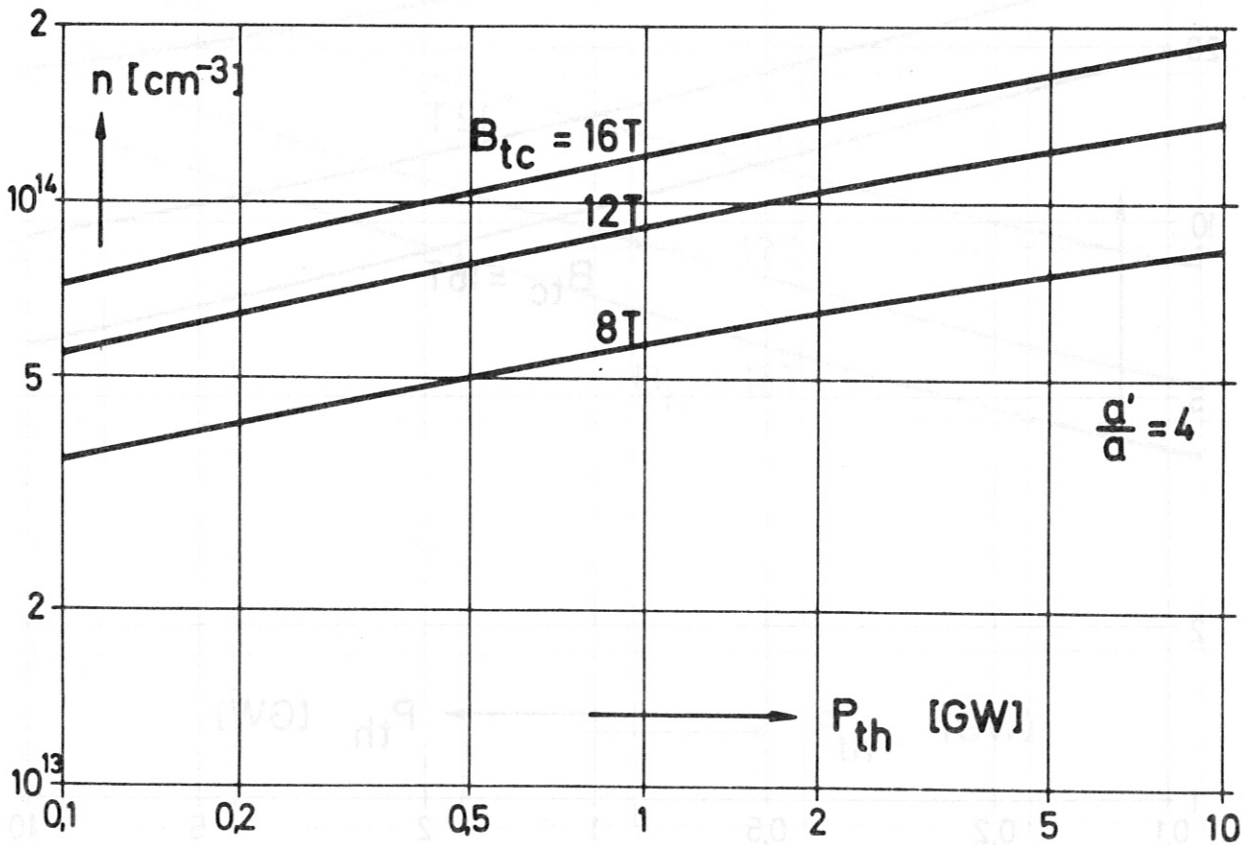
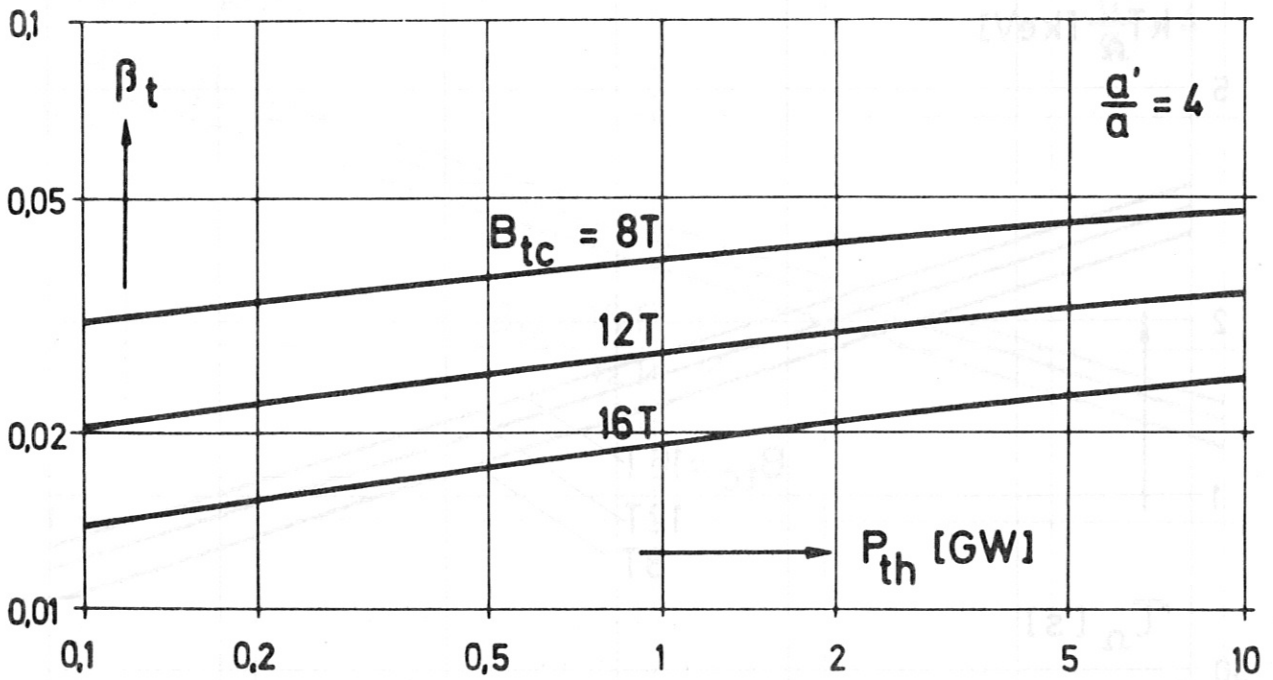


Fig. 11b β_t and plasma density vs. reactor power (ECS)

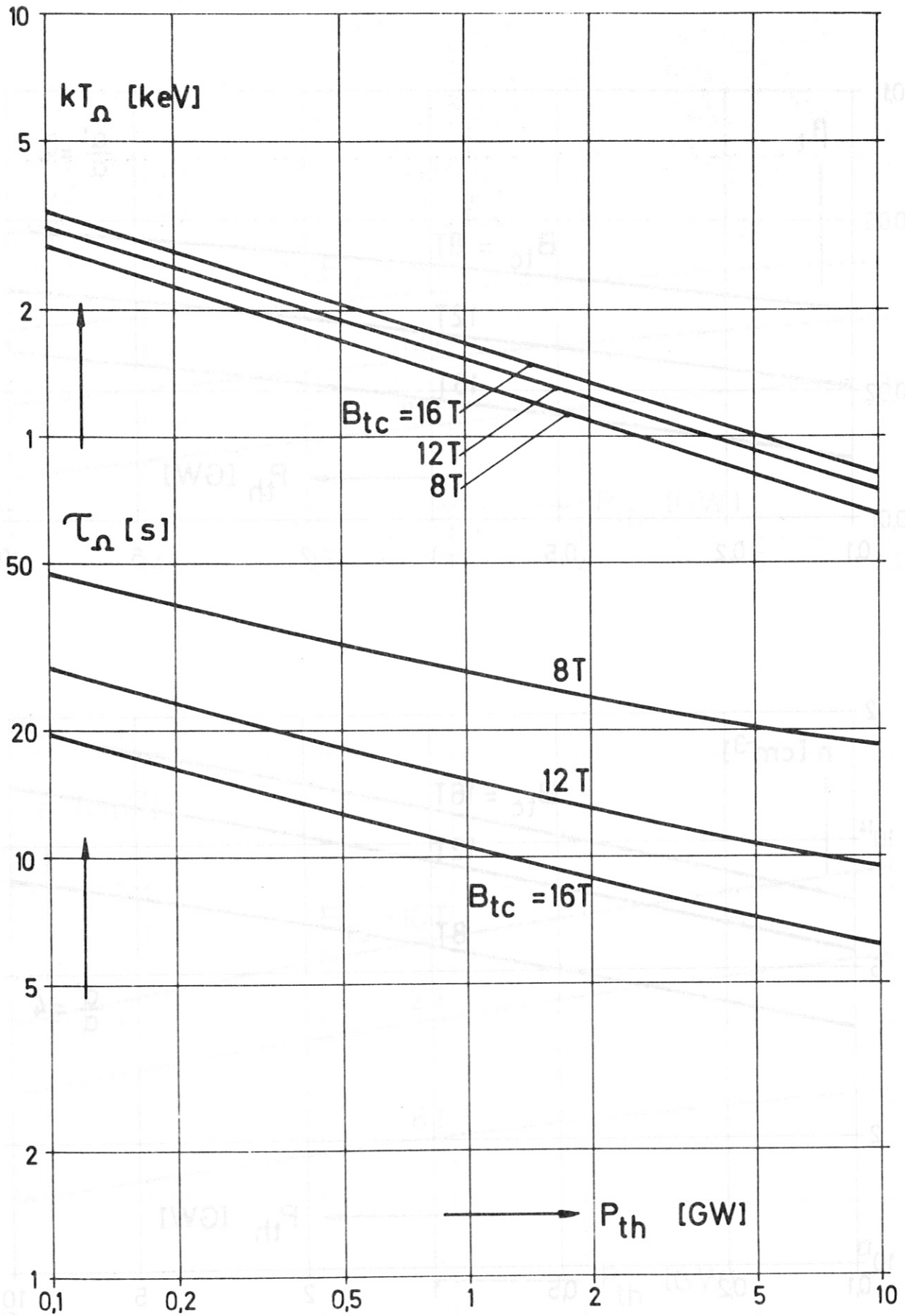


Fig. 12a Temperature by Ohmic heating and corresponding heating time vs. reactor power (CCS)

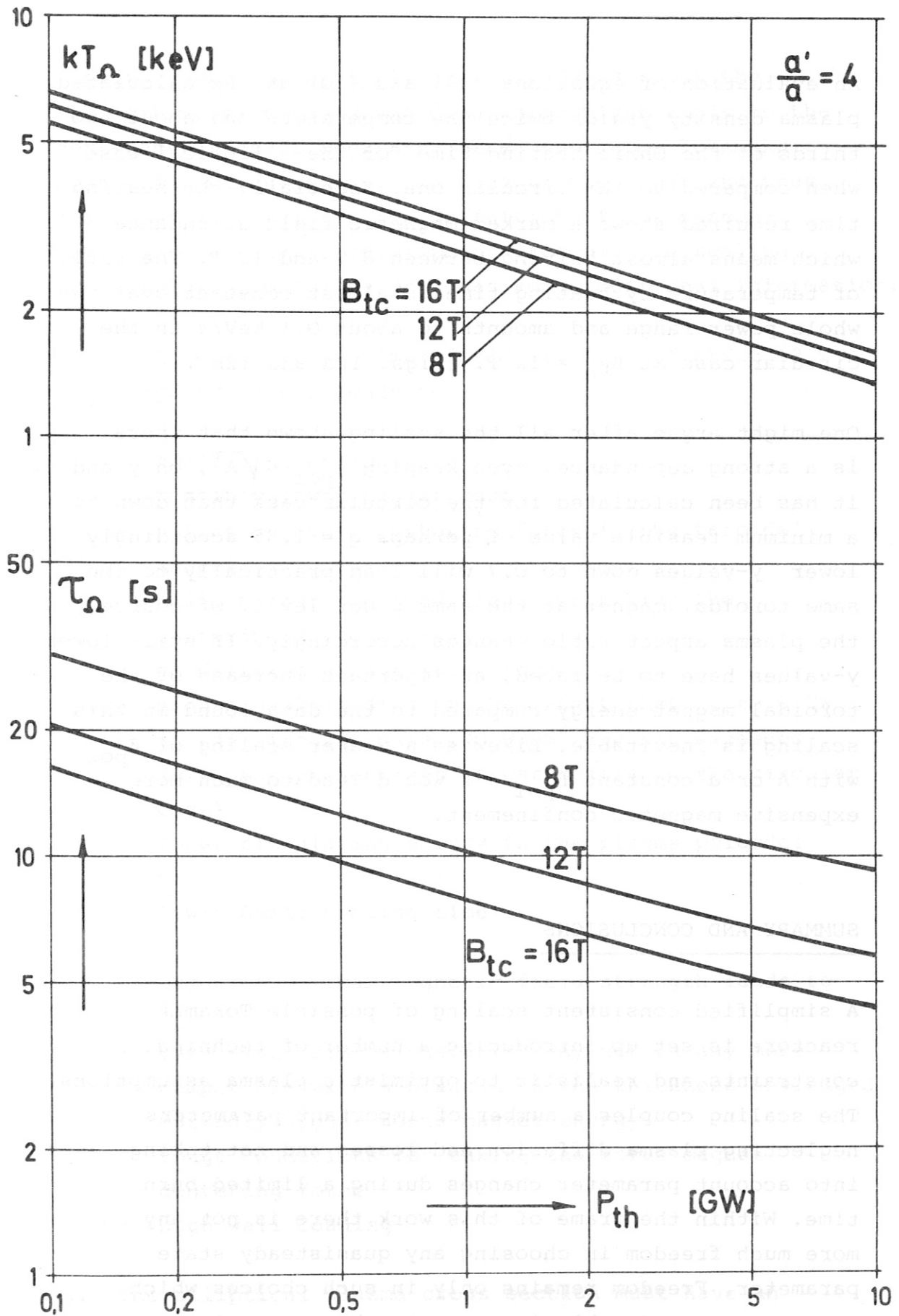


Fig. 12b Temperature by Ohmic heating and corresponding heating time vs. reactor power (ECS)

An evaluation of equations (29) and (30) at the calculated plasma density yields twice the temperature and about two thirds of the Ohmic heating time for the elliptical case when compared to the circular one. Especially the heating time required shows a marked magnetic field dependence which means almost halving between 8 T and 12 T. The ratio of temperature by heating time is almost constant over the whole power range and amounts to about 0.1 keV/s in the circular case at $B_{t_c} = 12$ T. (Figs. 12a and 12b).

One might argue after all the scaling shown that there is a strong dependence, even keeping $\beta_{pol} = \sqrt{A}$, on y and q . It has been calculated for the circular case that down to a minimum feasible value of perhaps $q = 1.85$ accordingly lower y -values down to 0.7 will lead practically to the same toroidal magnet at the same power level. Of course the plasma aspect ratio changes accordingly. If still lower y -values have to be faced, an important increase of the toroidal magnet energy compared to the data found in this scaling is inevitable. Likewise a weaker scaling of β_{pol} with A or a constant $\beta_{pol} = 1$ would lead to much more expensive magnetic confinement.

SUMMARY AND CONCLUSIONS

A simplified consistent scaling of possible Tokamak reactors is set up introducing a number of technical constraints and realistic to optimistic plasma assumptions. The scaling couples a number of important parameters neglecting plasma diffusion and losses and not taking into account parameter changes during a limited burn time. Within the frame of this work there is not any more much freedom in choosing any quasisteady state parameter. Freedom remains only in such choices which lead to a considerable increase in the toroidal magnetic energy required.

The lower end of the scaling at 0.1 GW is about the EPR machine size and gives data which might apply to the next generation of apparatus after the large Tokamaks being planned currently. The data at the lower end thus may be of interest for the definition of a superconducting torus magnet development program. The scaling towards larger machines provides some additional information:

1. An intermediate maximum field strength of about 12 T compared to 8 T leads to
 - smaller dimensions
 - possibly lower magnet cost
 - slightly higher centering force in the toroidal magnet
 - still manageable conditions for taking the centering force
 - no difference in tilting force
 - higher wall loading to the extent that up to 5 GW in the circular case 200 W/cm^2 are not exceeded (with the present set of parameters in the circular case)
 - lower circulating energy in the plasma poloidal field
 - lower Ohmic heating time

2. A very high maximum magnetic field strength leads to
 - very small dimensions which may not be any more compatible with a blanket of the thickness envisaged
 - markedly higher torus magnet energy
 - tough conditions for taking the torus magnet centering force
 - high wall loading

3. The elliptical plasma cross section must have an elongation at least of about 4 if an advantage in terms of β_t and plasma density is expected. In the case of

$a'/a = 4$ for any power the wall loading is higher than in the circular case and except for very high power levels the minimum toroidal magnet energy is larger.

4. In reality not the minimum energy torus magnets of circular or elliptical cross section will be used, but those with a force reduced cross section such as a practical D-shape. Thus the energies shown are lower limits. The choice of appropriate D-shaped magnets fulfilling the space requirements of poloidal divertor configurations and of accessibility and maintenance will be limited by the fact that force reduction couples the coil shape with the coil aspect ratio, ¹¹ a relation which is already set by the overall geometric scaling.

Of course, the considerations in this paper have to be further refined and the effects of different γ , q and β_{pol} scaling will be evaluated over a broader range. Preliminary calculations for $\beta_{pol} = 1$ have already shown that the principal scaling behaviour remains the same but at higher magnet energy levels for the same power.

A P P E N D I X

Here are some additional curves which originate from compiling the material given in the main report.

Figs. 13 through 16 refer to the circular case and the elliptical case with $\frac{a'}{a} = 4$.

Data for modest ellipticities using $\beta_t = \frac{1}{2} [1 + (\frac{a'}{a})^2] \cdot \beta_p$ will be given in a following report.

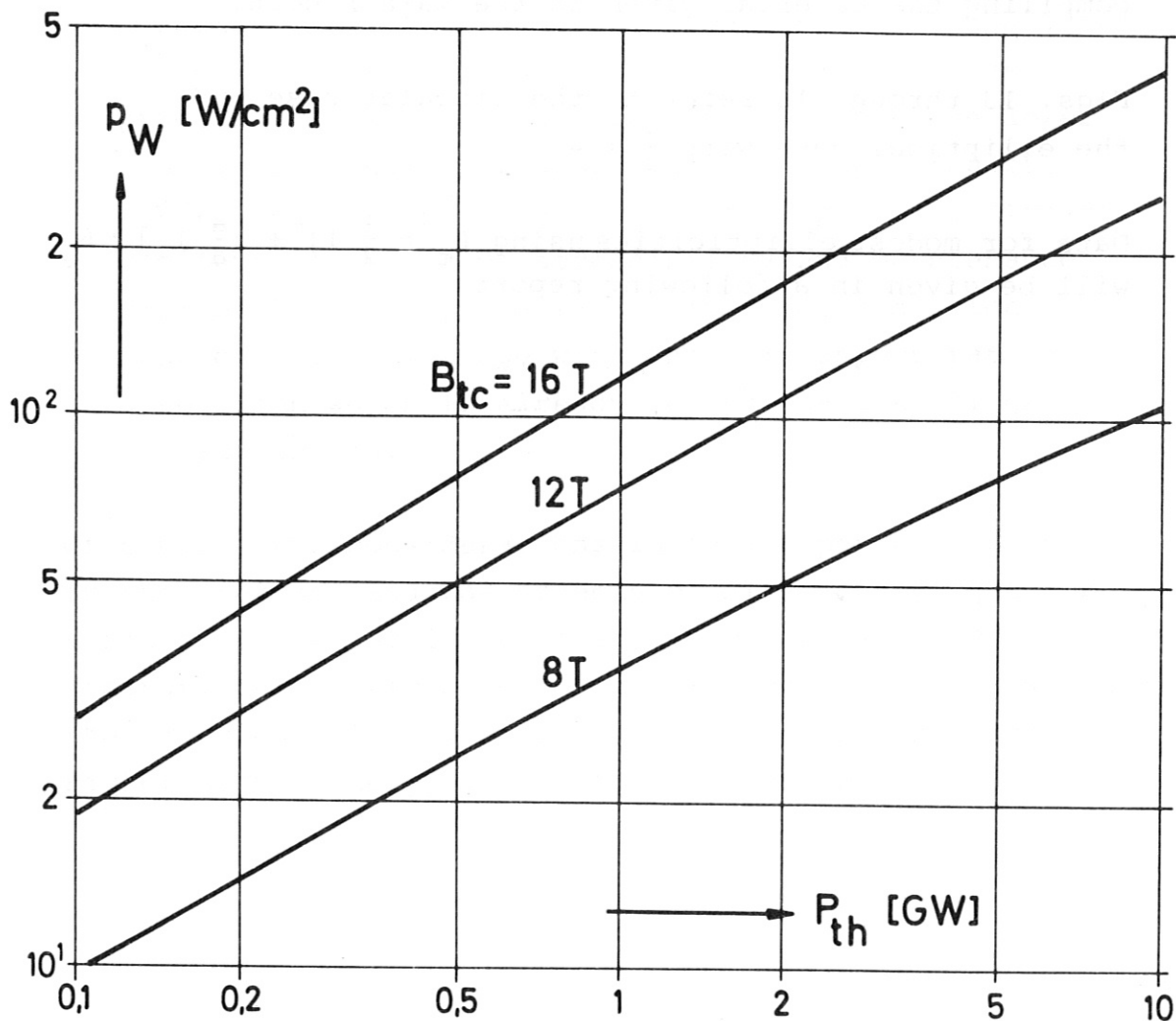


Fig. 13a Thermal power wall loading vs. reactor power (CCS)

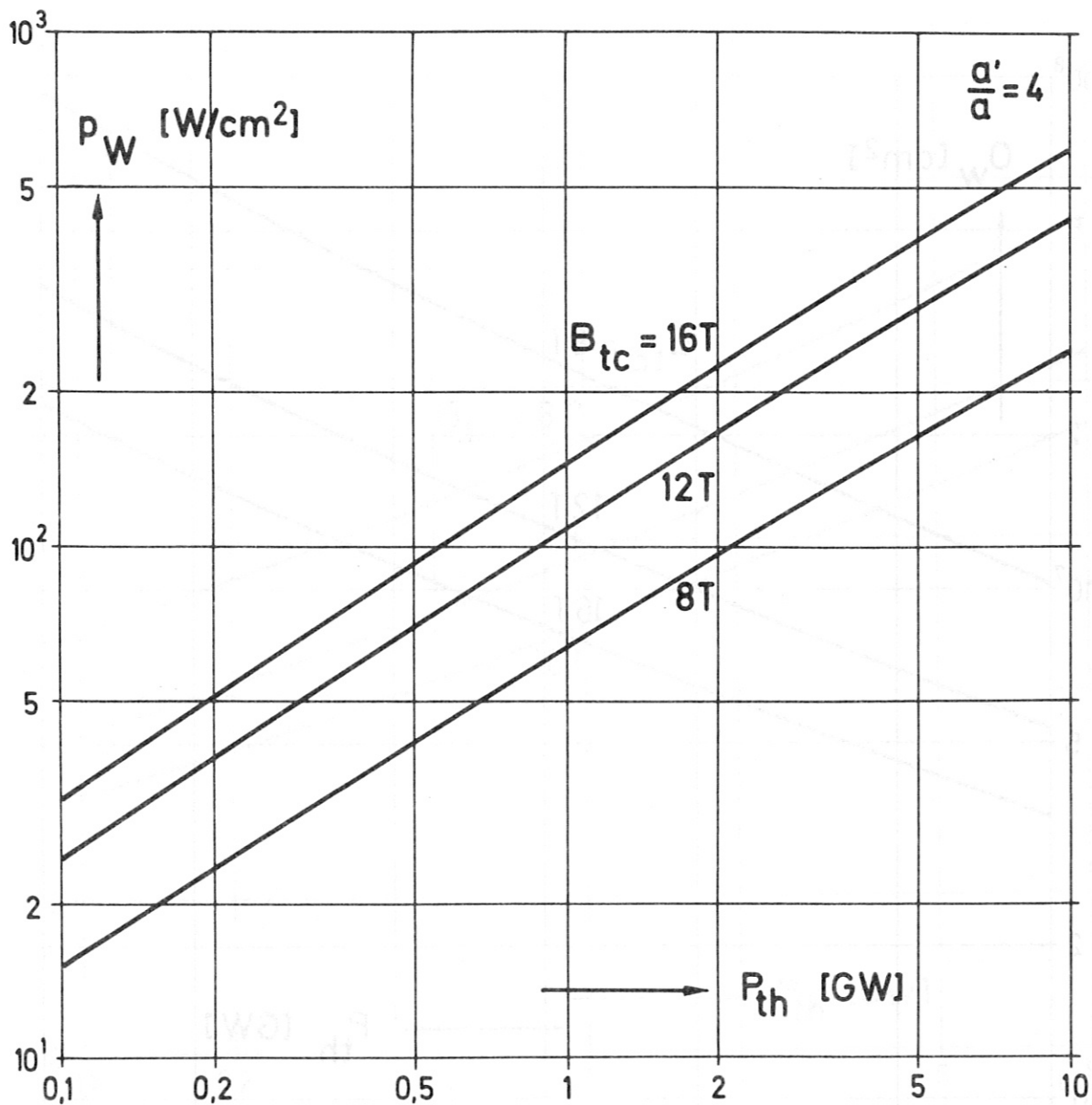


Fig. 13b Thermal power wall loading vs. reactor power (ECS)

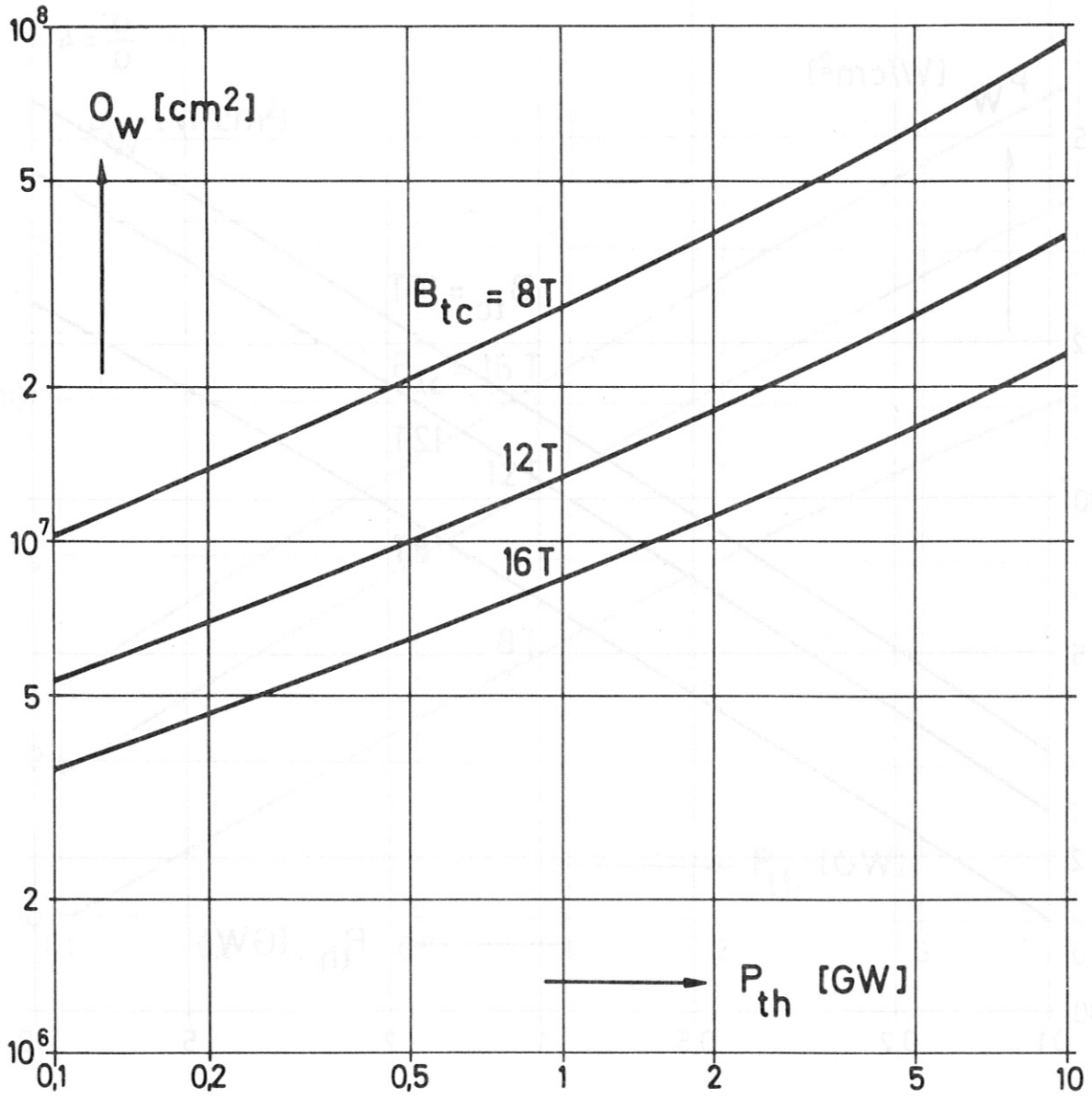


Fig. 14a Wall surface area vs. reactor power (CCS)

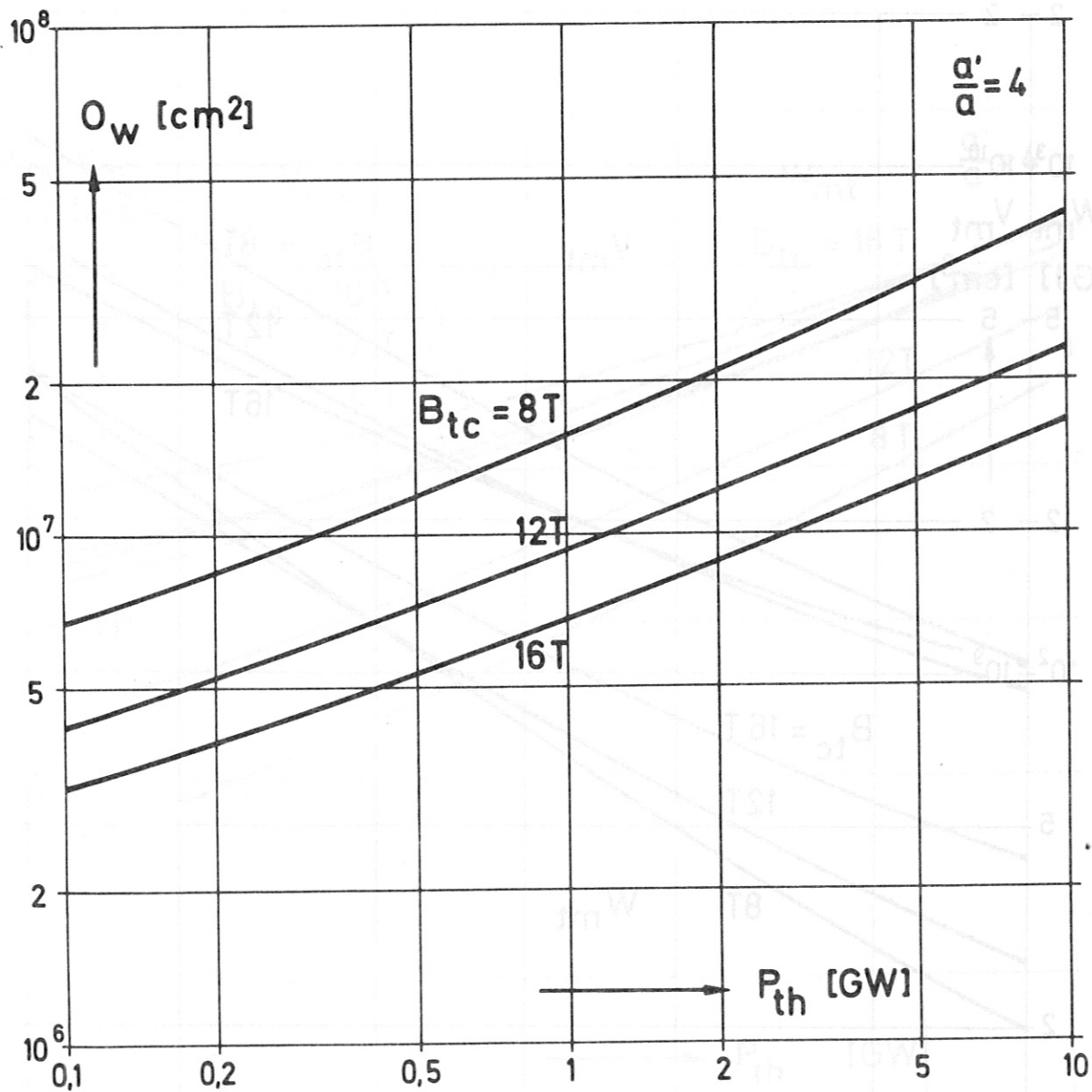


Fig. 14b Wall surface area vs. reactor power (ECS)

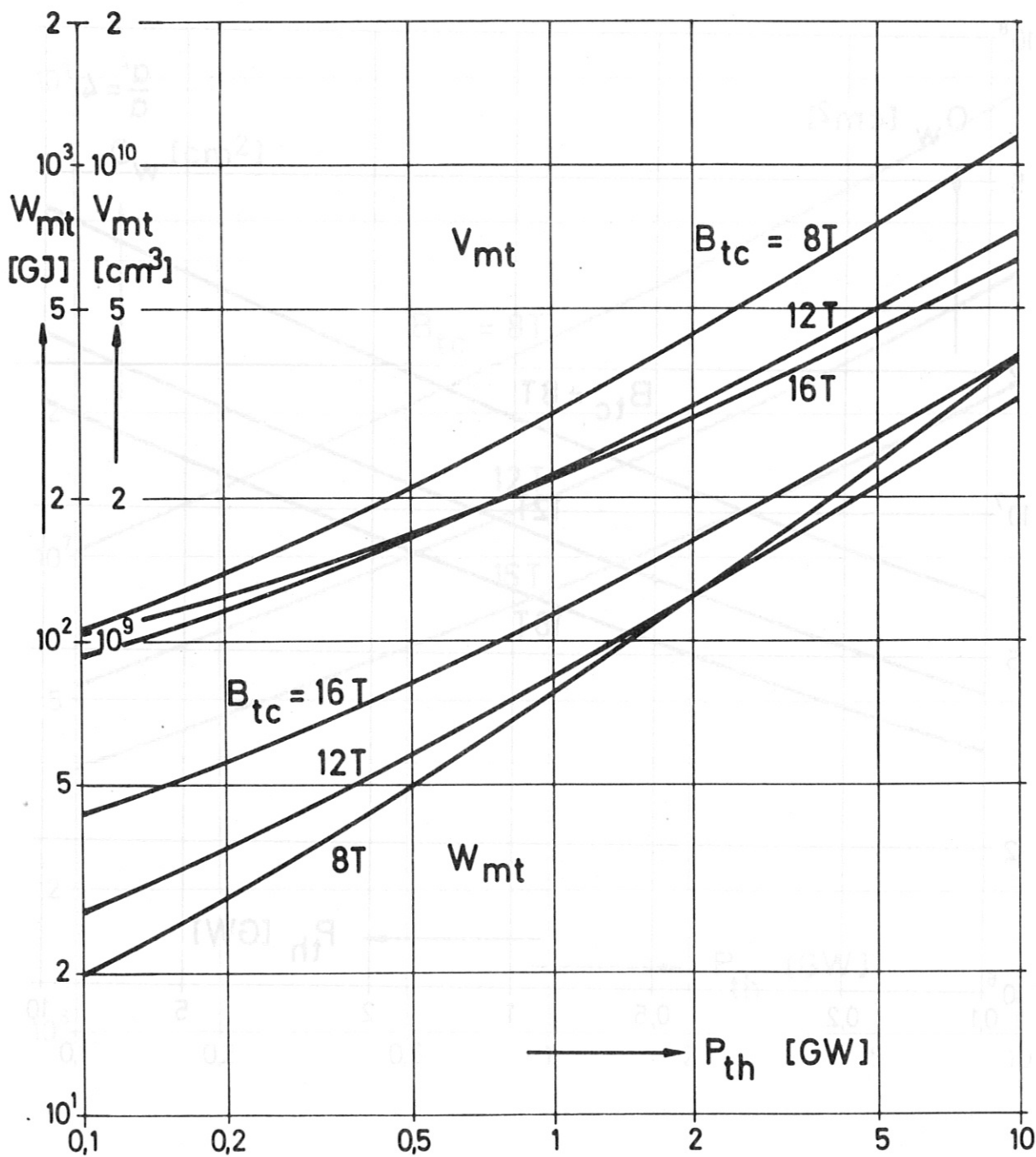


Fig. 15a Toroidal magnet winding volume and stored energy vs. reactor power (CCS)

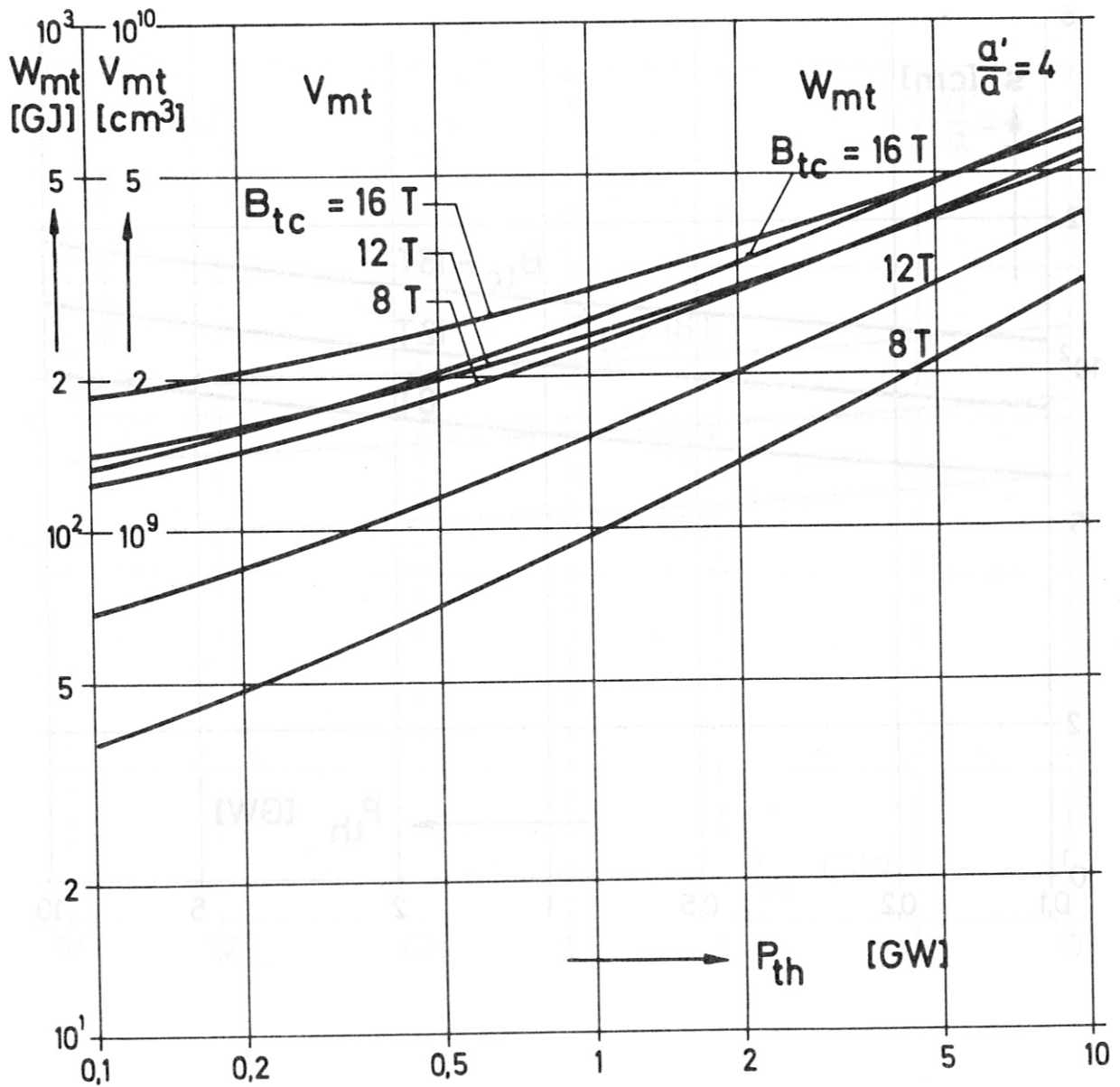


Fig. 15b Toroidal magnet winding volume and stored energy vs. reactor power (ECS)

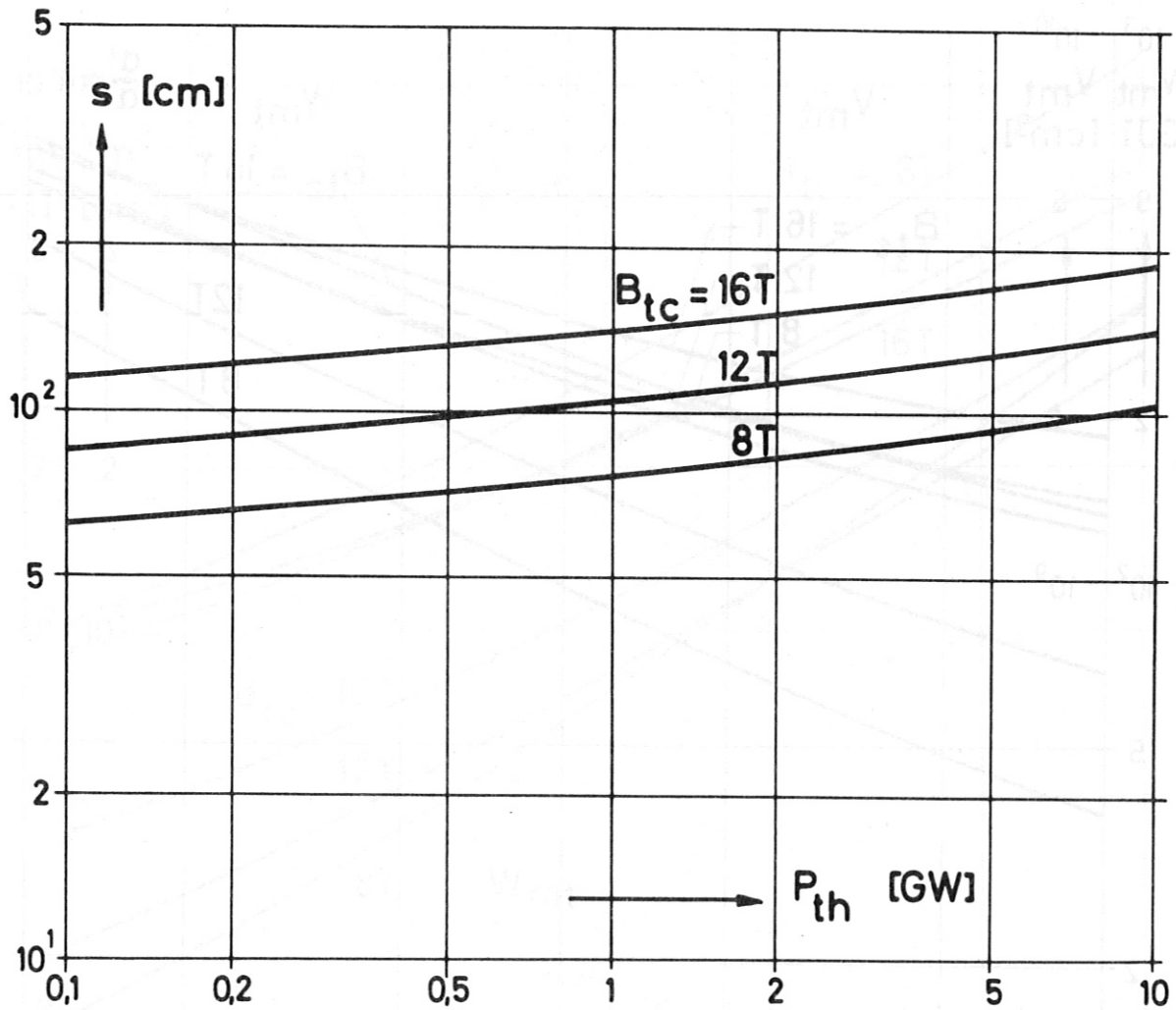


Fig. 16a Torus coils radial overall winding thickness vs. reactor power (CCS)

REFERENCES

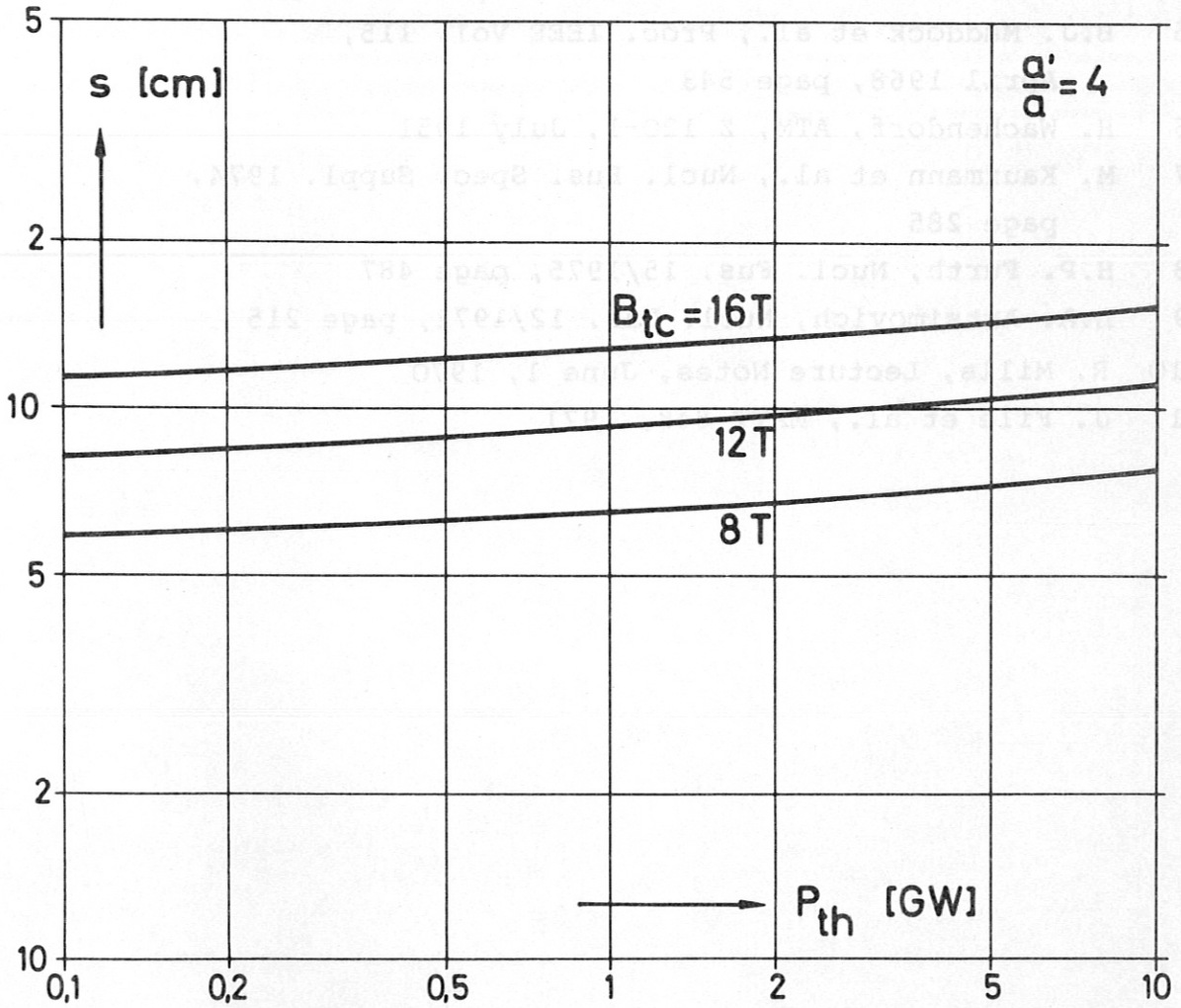


Fig. 16b Torus coils radial overall winding thickness vs. reactor power (ECS)

REFERENCES

- 1 A. Knobloch, EUR 4999e, page 181
- 2 J. Darvas et al, 6th Symp. on Eng. Probl. of Fus. Res., 1975, p. A1/5
- 3 F. Arendt et al, EUR 5182e, page 568
- 4 D. Düchs, Proc. EPS Lausanne 1975, Vol. 1, page 24
- 5 B.J. Maddock et al., Proc. IEEE Vol. 115,
April 1968, page 543
- 6 H. Wachendorf, ATM, Z 120-1, July 1951
- 7 M. Kaufmann et al., Nucl. Fus. Spec. Suppl. 1974,
page 285
- 8 H.P. Furth, Nucl. Fus. 15/1975, page 487
- 9 L.A. Artsimovich, Nucl. Fus. 12/1972, page 215
- 10 R. Mills, Lecture Notes, June 1, 1970
- 11 J. File et al., MATT 848, 1971